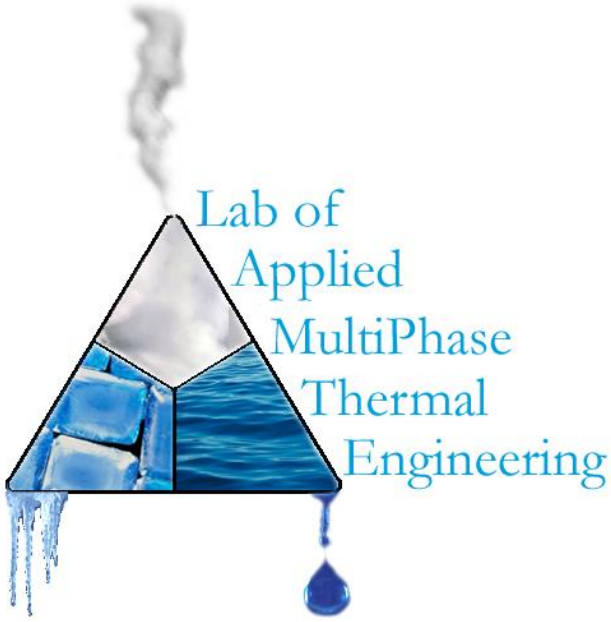

DALHOUSIE UNIVERSITY

Faculty of Engineering
Faculty of Science

Numerical Modeling of Tidal Turbine Behaviour under Real Turbulent Tidal Flow Conditions: Final Report

Prepared as part of an awarded
OERA Open Call
(Jan 1st 2016 – Dec 31st 2016)

By
Dr. Dominic Groulx, P.Eng, ing., Associate Professor
Tanguy Leroux
Nicholas Osbourne, MASc
Mechanical Engineering, Dalhousie University

Dr. Alex E. Hay, Professor
Justine M. McMillan, PhD Candidate
Oceanography, Dalhousie University

August 2016
Halifax, Nova Scotia, Canada

Executive Summary

In this research project, a numerical model and study, using fully transient simulations, of the turbulent flow over a generic 3-blade horizontal axis tidal turbine (HATT) subjected to real tidal flow inlet velocities, as captured in the lower Bay of Fundy (Digby area), was performed in order to determine the actual turbine behaviour under real turbulent tidal flow conditions. This numerical study shed more light on the findings from the Queen's University group as to the lowering of the turbine C_p and power production in a real tidal flow. The results of the simulations also provide additional insight into the wake dynamics and led to a comparison between steady flow wakes as studied previously and unsteady flow wakes encountered in real tidal flow environments.

The three objectives of this work were: 1)Develop a numerical model, using ANSYS CFX, enabling reliable study of unsteady turbulent flow over a horizontal axis turbine using real-life tidal flow data from the lower Bay of Fundy (Digby area), 2) Characterize the nature of the turbulent flow in the wake (length, zone of impact, strength of turbulence), and 3) Compare the unsteady results to the steady results obtained using the previously developed methodology in order to determine the impact on the turbine power and thrust values, and the wake behaviour.

A numerical model of a three bladed horizontal axis tidal turbine under realistic turbulent tidal flow was created. The results of this investigation have been compared with steady flow numerical model results with good agreement in trends. Prediction of both C_p and C_t are very similar in both cases. These similar trends observed in both C_p and C_t curve are important as they indicate that the appropriate flow physics are being accounted for. Only TSR values related to maximum C_p and C_t changed. For maximum C_p, tip speed ratio is approximately equal to 3.9 in steady flow and 4.1 for transient conditions. In transient flows, this results however in an approximate 4% reduction in performance (for TSR = 3.5), though there is increased uncertainty due to the levels of scatter in the numerical data points.

Velocity deficit plots show the wake is wider in transient simulations than steady ones. The velocity deficit disappears also faster in the constant velocity simulations. Turbulent effects in the wake seem to increase after a distance of 10D downstream of the turbine in this setup. These turbulence effects are higher in the transient simulations.

This comparative analysis of numerical steady and transient simulations shows the impact of the unsteadiness of realistic tidal flows on the performance of tidal turbines. Based on these results, the current use of steady state testing (numerical or experimental) for design stage can be questioned. The observed changes in the wake's characteristics and the high variations of the loads on the blades (reference to C_t-curve as a function of time) must also be better assessed.

Table of content

List of figures

List of tables

List of Abbreviations and Variables

Greek Letters

ρ	Fluid Density [kg/m^3]
κ	Von Karman constant
ν_*	Friction velocity [m/s]
ω	Rotational Velocity [rad/s]

Variables

A	Turbine Swept Area [m^2]
C_P	Power Coefficient
C_T	Thrust Coefficient
D	Turbine Diameter [m]
k-ε	Turbulent Kinetic Energy – Turbulent Dissipation (Turbulence Model)
k-ω	Turbulent Kinetic Energy – Specific Dissipation (Turbulence Model)
P_m	Power [W]
P_{rel}	Relative Pressure [Pa]
Q	Torque [Nm]
R	Turbine Radius [m]
S	Turbulence Spectral Density [N m/kg]
t	Time [s]
T	Thrust [N]
TI	Turbulence Intensity
TSR	Tip Speed Ratio
v'	Turbulent velocity component [m/s]
V	Velocity [m/s]
V_A	Average velocity over the turbine swept area [m/s]
$\bar{V}$	Mean Velocity [m/s]
$V_{deficit}$	Velocity Deficit
V_{in}, V_0	Inlet Velocity [m/s]
V_W	Velocity in the wake [m/s]
X	Horizontal distance either side of the turbine [m]
y^+	Dimensionless Wall Distance (Y plus)
Y	Vertical distance from the sea bed [m]
Y_0	Sea bed roughness length scale [m]
Z	Distance downstream from the inlet [m]

1 Introduction

The information contained hereof has been prepared by the Laboratory of Applied Multiphase Thermal Engineering (LAMTE) to report on work done between January 2016 and July 2016 as part of an OERA grant funded research. This research involves the investigation of turbine and wake behaviour under real turbulent tidal-flow over a horizontal axis tidal turbine (HATT).

To fully understand the importance of performing this research project, some background must be given to put it into a broader context. Today, still, the vast majority of experimental tests and numerical models of tidal turbine are done in constant velocity towing tank or flume tank (experimental) or using constant inlet velocity conditions with randomly generated turbulence intensity (numerical). Both tools have been, and continue to be, used for tidal turbine design, optimization and characterization; providing easy to obtain and repeatable data. However, recent results presented by Dr. Bjorn Elsaesser's group from Queen's University Belfast showed that the turbine maximum operating C_p is reduced by 24%, with a consequential reduction in power production of 30%, when comparing turbine operation in a real unsteady tidal flow to steady tests performed by pushing the turbine in still water [1]. This initial result has been found experimentally and now requires further studies both in real tidal flow and in numerical models.

The aforementioned results from the Queen's University group point to the fact that most turbine developers, relying on steady tests, might be overestimating their turbine power rating by tens of percent; which will have an important impact on the overall financial assessment and economic viability of tidal projects. Real tidal flow tests are expensive to run and very few tidal turbine companies have reached this testing stage. Furthermore, numerical models for the most part cannot be built using "real tidal flow" data since such small scale, high-frequency data has not been available in the past.

The researchers at Dalhousie University found themselves in an interesting position to start studying this problem since in the last 3 years, through projects funded in part by OERA, a methodology for numerical modeling using CFD of turbulent flow over tidal turbine was established [2, 3] (OERA Unsolicited Grant – 2013), and real tidal flow data from Grand Passage, Digby Neck was captured in-situ experimentally [4, 5] (OERA Grant 2011; NSERC ENGAGE Grant 2013).

1.1 Purpose

In this research project, a numerical model and study, using fully transient simulations, of the turbulent flow over a generic 3-blade horizontal axis tidal turbine (HATT) subjected to real tidal flow inlet velocities, as captured in the lower Bay of Fundy (Digby area), was performed in order to determine the actual turbine behaviour under real turbulent tidal flow conditions. This numerical study shed more light on the findings from the Queen's University group as to the lowering of the turbine C_p and power production in a real tidal flow. The results of the simulations also provide additional insight into the wake dynamics and led to a comparison between steady flow wakes as studied previously [3] and unsteady flow wakes

encountered in real tidal flow environments. This investigation addresses OERA's Marine Renewables Energy Research Targeted Research Priorities 4 and 5:

4. Monitoring and Optimizing Operational and Life-Cycle Performance of Turbines and Related Equipment: As will be shown in the literature review and innovation section, it is now starting to be understood that the unsteadiness in real tidal flow, compared to steadier experimental tank test, leads to different energy capture and production from tidal devices (with energy production reduction of up to 30%), as well as different turbine/blade load and wake physics. With each tidal site being different in the nature of the flow and the bathymetry, specific transient simulations directly coupled with real data from the site of interest provide a more accurate modeling tool for design and turbine characterization. Very few of those numerical studies have been performed worldwide, and none in North America so far as we are aware.

1.2 Literature Review

As stated by tidal turbine manufacturers (Alstom), *measuring the performance of a tidal turbine presents two key challenges to the tidal energy industry: 1) Prediction in the design stage; 2) Verification of the performance once operational* [6]. Prediction in the design stage is currently done through small-scale steady state experimental testing, which uses constant velocity towing tank [7, 8] or flume tank [9] to determine power produced and thrust acting on the designed turbine; or a numerical model of the turbine over which the turbulent flow is simulated using either a simpler blade element/momentum (BEM) [10, 11] method, actuator disks representations [12] or the more powerful and accurate computational fluid dynamics (CFD) methods [13]. Large emphasis is given to this first stage since stage 2 (verification of the performance once operational) has only been undertaken by a select few turbine developers (Alstom through 4 years of careful measurement and testing [6], OpenHydro through years at EMEC and MCT with their operational Strangford Lough turbines); however, OpenHydro still performs their stage 1 numerical study using steady, constant velocity conditions [14].

The heavy reliance of today's turbine developers on steady-flow testing (either experimental or numerical) combined with the findings of the Queen's University group that testing of a turbine in steady-flow could lead to an energy generated over prediction of up to 30% [1] is a direct indication of the need for a movement towards the study of unsteady effects and unsteady testing; the nature of the flow encountered between a steady-flow test and a real-tidal unsteady flow also clearly illustrate the need for stronger unsteady study as seen in Fig. 1 [15].

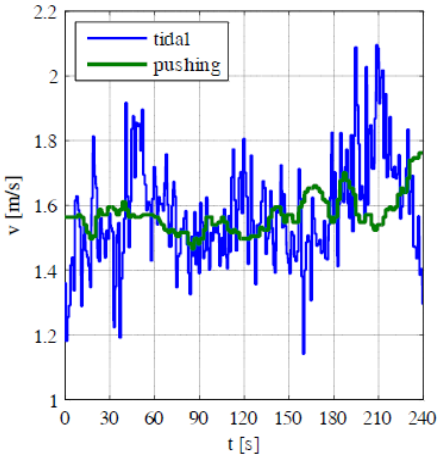

Figure 1 Time series (4 minutes) of velocity seen by a turbine in a steady-flow test (pushing in this case) and unsteady tidal flow test.

Of the various numerical methods that are employed today for studying turbulent flow over turbines, very few can be employed to study unsteady flow with high enough accuracy. Blade element/momentum (BEM) [10, 11] methods have been shown to be insufficient for unsteady loading [16]. The actuator disc method still lacks the solution quality that would result from a standalone CFD model. A CFD approach has been shown to have the capability of resolving turbulence in the near and far field regions at fine resolutions for a three dimensional horizontal axis tidal turbine [17]. The most commonly used turbulence model in the field of tidal turbine simulation today is the Shear Stress Transport (SST) model. The SST model utilizes k-ω in the inner boundary regions and k-ε in the free stream regions, and is capable of resolving turbulence within an acceptable margin of error [18, 19].

This shift into unsteady studies has started recently with numerous papers in the last two years looking at various engineering aspects, for example: CFD study of the load on turbine blades stemming from unsteady tidal flow [20], experimental study in a circulating tank of unsteady turbulence (generated artificially using static grids) effect on a small-scale tidal turbine [9, 21, 22]; these studies however used randomly generated flow field and turbulence level. Only one recent conference paper from a team at the University of Manchester (UK) shows the integration of "real tidal" velocity data as the inlet condition of a CFD simulation to properly study the impact of unsteadiness in the flow, in this case using data from the EMEC test site in the Orkney Isles [19].

In Canada, work on characterizing the unsteadiness of tidal flows in the Bay of Fundy has been underway for some years [4]. On the numerical side, high-fidelity simulations of the unsteady flow in Minas Passage have been performed by the team at UNB [23]. On the observation side, direct measurements of turbulence in Minas Passage are so far lacking. Reliance instead is on the available measurements using commercially available acoustic Doppler current profilers (ADCPs) [22]. These measurements are now somewhat dated, as the Doppler technology used was not the most accurate even at the time. Nevertheless, the results in [5] indicate that data from standard commercially-available ADCPs can be used to obtain representative estimates of second-order turbulence statistics, including the turbulent kinetic energy and the rate of energy dissipation [24].

This research project aims to incorporate real tidal flow data to numerical turbulent CFD simulations of HATT in order to determine the actual turbine behaviour under real turbulent tidal flow conditions, shedding more light on the findings from the Queen's University group as to the lowering of the turbine

C_p and power production in a real tidal flow. Towards the accomplishment of this project, a numerical methodology as already been developed and tested in a previous OERA funded project. The methodology was validated against experimental results [7] and used to study turbine wake characteristics [3]. Using this methodology as the starting point for this project, the tidal flow data collected by Dr. Hay's group as reported in the previous paragraph will be used to create the first ever numerical study of turbulent flow over tidal turbine representative of Bay of Fundy unsteady conditions.

2 Scientific Objectives

As defined in the original grant application, the three objectives of this work were:

1. Develop a numerical model, using ANSYS CFX, enabling reliable study of unsteady turbulent flow over a horizontal axis turbine using real-life tidal flow data from the lower Bay of Fundy (Digby area);
2. Characterize the nature of the turbulent flow in the wake (length, zone of impact, strength of turbulence);
3. Compare the unsteady results to the steady results obtained using the previously developed methodology [2] in order to determine the impact on the turbine power and thrust values, and the wake behaviour.

The success of this project will allow for improved understanding of the unsteadiness effect on turbine operation and energy production; both factors greatly contributing to the economics of and risks to the tidal energy industry.

3 Methodology

3.1 Turbine Geometry Validation

The validation of this geometry is presented in [25] and was performed in the summer of 2015 by Grant Curie, an undergraduate researcher working at the LAMTE under the supervision of Nicholas Osbourne. The turbine geometry was developed to match as closely as possible the experimental turbine used by Doman *et al.* [8]. Table 1 presents the experimental geometry of the NREL S814 airfoil shape blades. The blade twist axis of rotation is located at 25% of the chord length from the leading edge for each cross section. The blade profiles were exported and lofted in SolidWorks to create the three dimensional geometry shown in Fig. 2. The hub pitch angle for the experimental turbine was measured to be 28 ± 0.875°, and 28.875° was used in the numerical model. The nacelle and support structure geometries were estimated from reviews of the publications, dimensions of which are provided in Table 2. The blade roots and rotor hub were greatly simplified from the experimental setup to facilitate meshing.

Table 1 Blade Parameters [8]

Radius (m)	Twist (°)	Chord (m)
0.089	0	0.0643
0.114	-4.38	0.0629
0.149	-10.74	0.0598
0.183	-14.80	0.0560
0.216	-17.33	0.0516
0.251	-18.91	0.0473
0.286	-19.75	0.0426
0.321	-20.39	0.0381
0.355	-20.87	0.0337
0.381	-21.11	0.0249

Table 2 Nacelle Geometry Dimensions

Parameter	Dimension
Nacelle Length (tip to tip)	1700 mm
Rotor Diameter	150 mm
Rotor Depth	700 mm

Tow tank tests were completed at the Kelvin Hydrodynamics Laboratory tow tank at Strathclyde University [8]. Table 3 presents the dimensions of the facility. These parameters are represented in the numerical fluid domain with the exception of the domain length. The domain length was shortened to 22*D*, with inlet and outlet lengths of 2*D* and 20*D* respectively, where *D* = 0.762 mm denotes the turbine diameter. Figure 3 illustrates the fluid domain shortened up to 7*D* to show more of the turbine area. It has been shown that this length is sufficient as the near wake physics and performance of the turbine is not significantly affected by the outlet domain length [2].

Figure 2 Turbine rendering

Table 3 Tow Tank Parameters [8]

Parameter	Magnitude
Length	76 m
Breadth	4.6 m
Height	2.5 m
Maximum Flow Speed	5 m/s

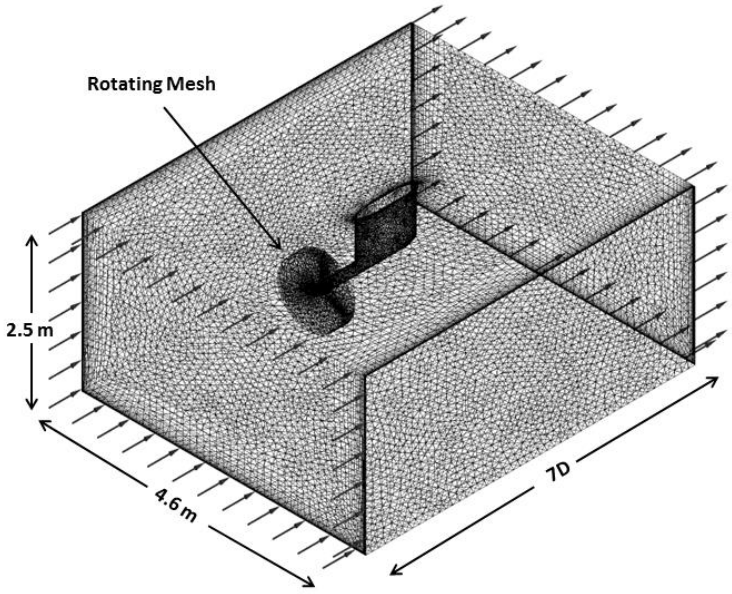

Figure 3 Fluid domain

The Shear Stress Transport (SST) turbulence model was chosen for this investigation as it has been proven to have an acceptable balance between accuracy and computational effort [26]. SST is a two equation eddy viscosity model comprised of the *k-ε* and *k-ω* models. An inherent transitional regime is used that applies *k-ω* in the inner boundary layer and *k-ε* when further in the free-stream. This approach negates the shortcomings of the individual models. A final comparative study, as part of the remaining work, will show the difference in results from these three models (*k-ε*, *k-ω*, SST).

A complete mesh convergence study was completed as presented in [25]; a detailed view of the mesh around each turbine blade, including the inflation layer around the blade, is presented in Fig. 4. Using the final mesh, frozen rotor, steady-state simulations are four different inlet velocities (0.5, 0.8, 0.9 and 1 m/s) over a range of tip speed ration (TSR) were performed in order to determine both the power (C_p) and thrust (C_t) coefficients for the turbine. The mathematical definition of all three terms are presented in Eqs. (1) to (3).

$$TSR = \frac{\omega R}{V} \tag{1}$$

where ω is the rotational rate in rad/s, R is the turbine radius (381 mm), and $\bar{V}$ is the reference velocity (constant during the experiment).

$$\boldsymbol{C_p = \frac{P_m}{\frac{1}{2}\rho A V^3} = \frac{\omega Q}{\frac{1}{2}\rho A V^3}} \tag{2}$$

$$\boldsymbol{C_t = \frac{T}{\frac{1}{2}\rho A V^2}} \tag{3}$$

where T and P_m are the thrust and mechanical power produced, respectively, ρ is the fluid density, A is the rotor swept area, and Q is the rotor torque.

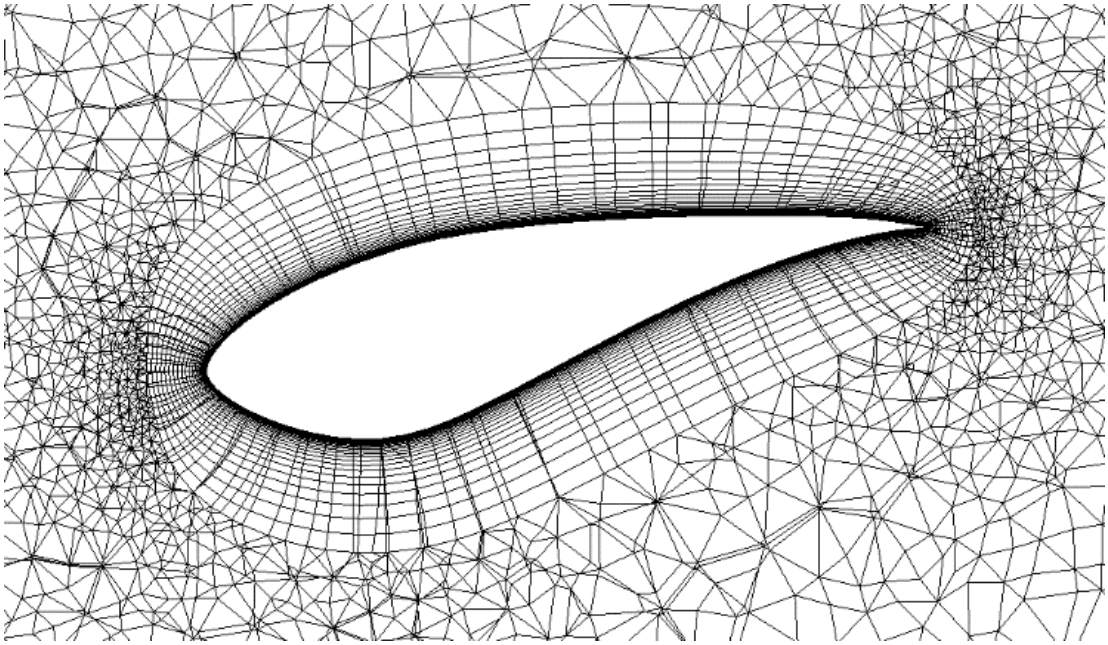

Figure 4 Detailed view of the blade inflation layer

Finally, the results of those simulations were compared to the experimental results that were obtained during two tank testing [8]. Both numerical and experimental results are plotted in Figs. 5 and 6.

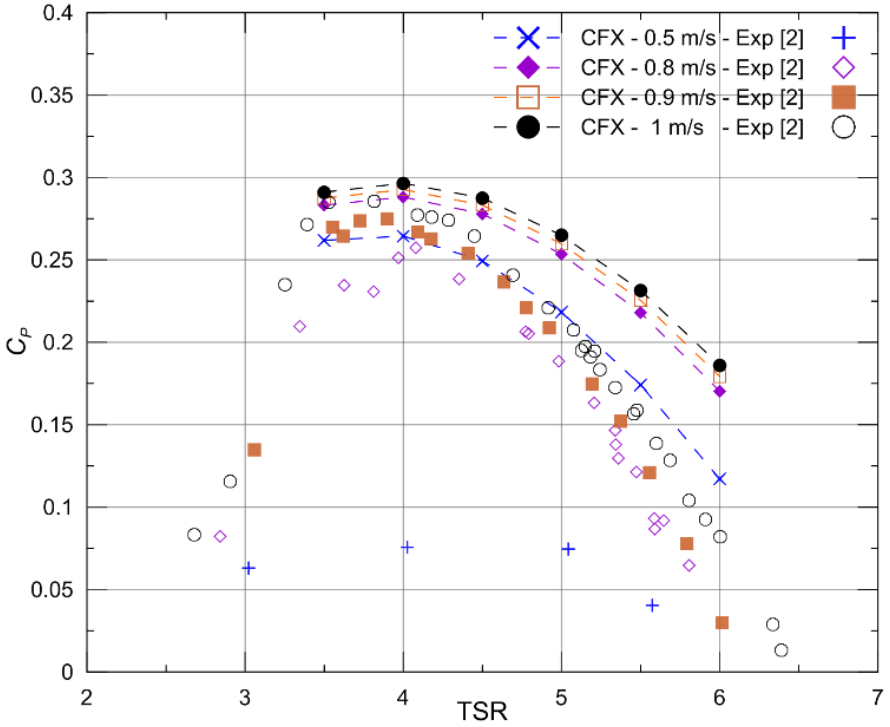

Figure 5 Numerical C_p as a function of TSR for four inlet velocities compared to the experimental measurements [8].

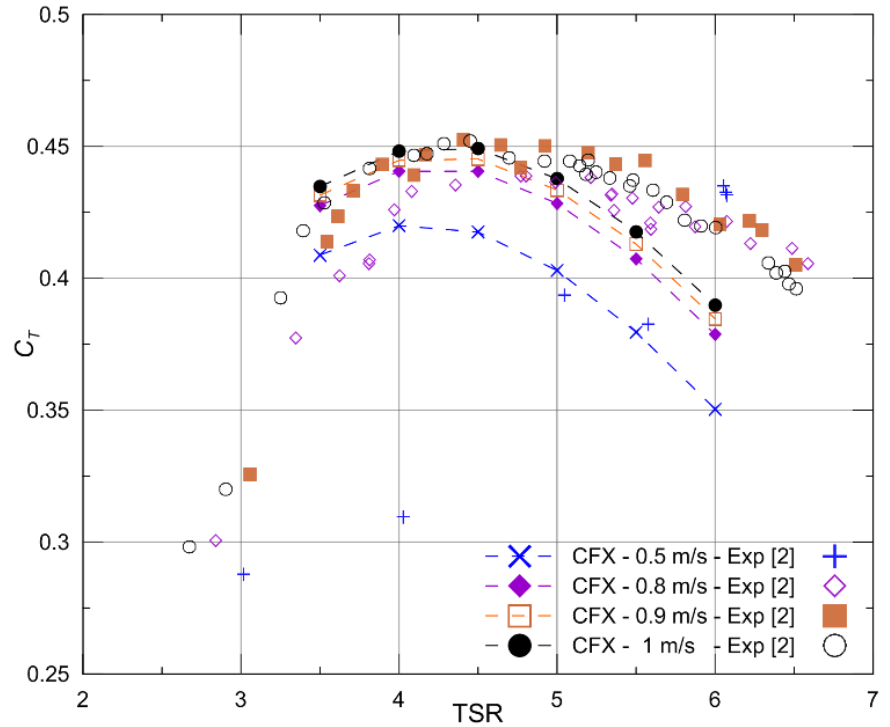

Figure 6 Numerical C_t as a function of TSR for four inlet velocities compared to the experimental measurements [8].

As can be seen from Figs. 5 and 6, experiments where performed starting at TSR as low as 2.6 where very poor performance was obtained. Since the fluid dynamics causing this poor performance was not included and model in the CFD simulations, numerical results starting at a TSR of 3.5, at which point the turbine performed as expected, are included.

The numerical results for C_p are generally in good agreement with the experimental results, especially for the fastest flow velocities and in the rage of TSRs from 3.5 to 5 during peak performance of the turbine. At higher TSRs, a clear over prediction is observed. Again, additional flow physics are in play at higher rotational rates (separation, potential cavitation) which are not accounted for at this time in the simulations.

The correlation of C_t is in better agreement compared to the experimental results and over a wider range of TSRs. However, there is a slight under prediction at high TSRs for reasons similar as those listed at the end of the previous paragraph; the occurrence of cavitation at high TSRs has been shown to greatly reduce power capture [27].

Deviations of both C_p and C_t at high TSRs from experimental results could also be attributed to the inaccuracies in the modelled turbine geometry. The simplifications made to the blade roots and rotor hub are thought to result in an increase of power capture. Also the chosen hub pitch angle of 28.875° compared to 28 ± 0.875° of the experimental turbine would also increase the angle of attack and thus power capture. The quality of the manufactured blade and the trailing edge treatment is unknown, and would have a significant effect on the results. The uncertainty in experimental C_p, particularly at high TSRs, could account for some of the over-prediction.

With all these factors taken into consideration, the numerical results are deemed acceptable.

3.2 Additional Wake Results from the Steady-State Validation

Additional results from the simulations are worth looking at, noting that in order to get a better sense of the wake, those results were obtained running the steady-state simulations to 2500 iterations. Figure 7 presents a side view of the wake, specifically looking at the normalized velocity for three simulations at a TSR of 4.5 with inlet velocities of 0.5, 0.8 and 1 m/s. It is interesting to note that the wake takes a very similar shape irrespective of the inlet velocities, with velocity reduction to 75% of the inlet velocity still observed at the end of the simulation domain (20*D*).

Similar wake as a function of inlet velocity can also be observed in Fig. 8 showing three wakes seen from the side for TSR = 6. In this case, it appears the wake disappears before reaching the 20*D* end of the simulation domain. It is important however to note that for higher TSRs, it appears an even larger number of iterations is required to obtain a fully steady-state solution; therefore, this disappearance of the wake is more than likely a result of the limited 2500 iterations used, a problem that should be solved when running transient simulations, as done through this research project.

Figure 9 shows a view of the wake seen from the top. Results were all similar irrespective of the TSR or inlet velocity used. It is still interesting to observe that the velocity wake never extends larger than the diameter of the turbine rotor in the horizontal direction.

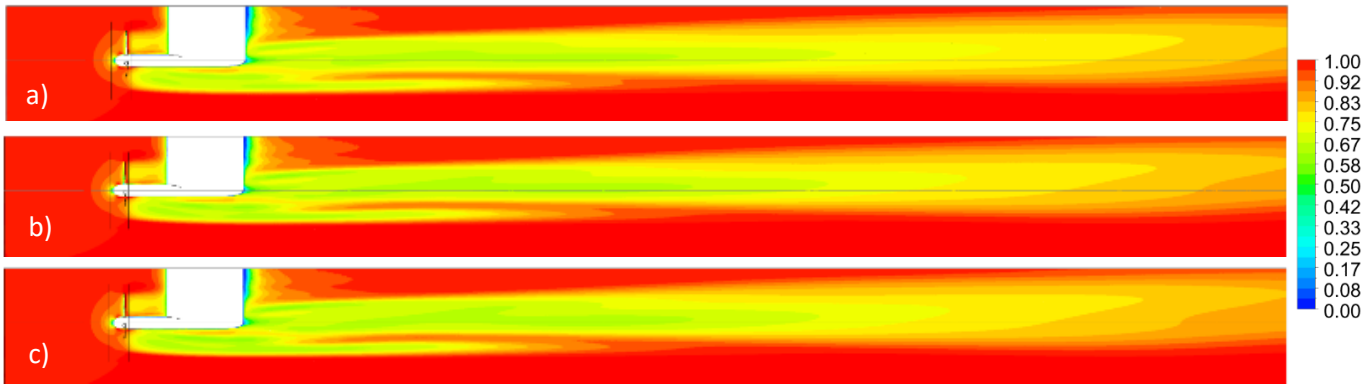

Figure 7 Normalized velocity V/V_{in} in the wake seen from the side on a plane crossing the middle of the turbine for TSR = 4.5: a) V_{in} = 0.5 m/s,b) V_{in} = 0.8 m/s and a) V_{in} = 1 m/s

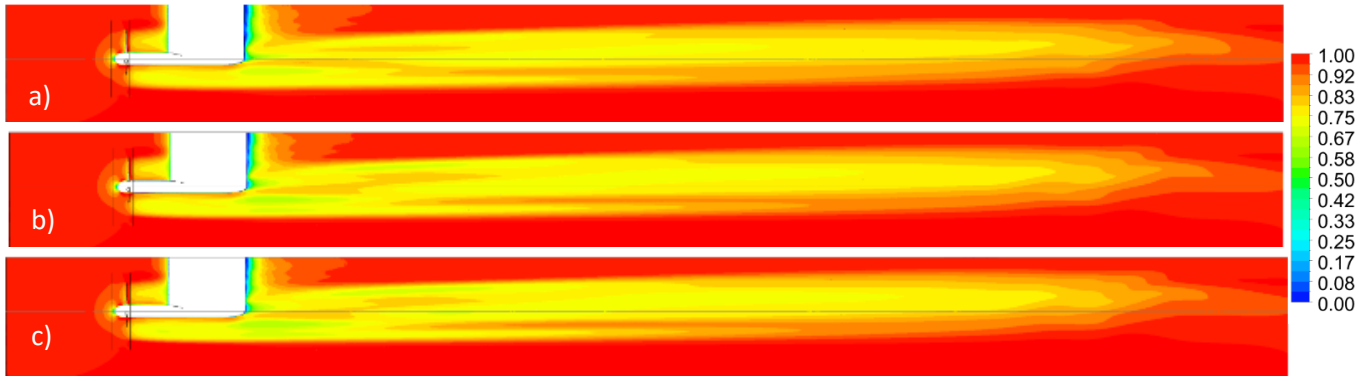

Figure 8 Normalized velocity V/V_{in} in the wake seen from the side on a plane crossing the middle of the turbine for TSR = 6: a) V_{in} = 0.5 m/s,b) V_{in} = 0.8 m/s and a) V_{in} = 1 m/s

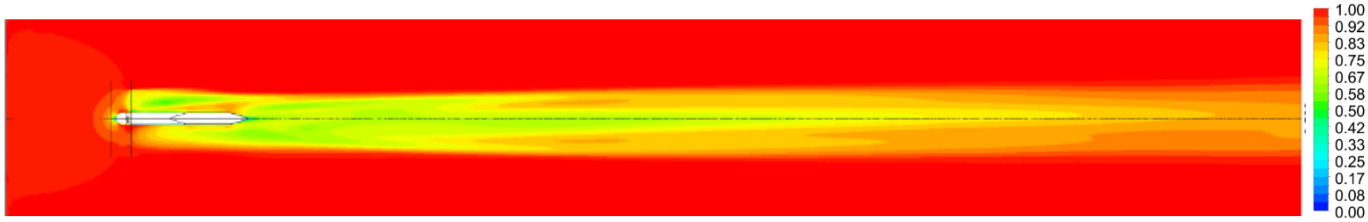

Figure 9 Normalized velocity V/V_{in} in the wake seen from above on a plane crossing the middle of the turbine for TSR = 4.5 at V_{in} = 1 m/s

3.3 Transient Turbulent Modelling

In order to perform the transient turbulent studies required for this project, transient both in the nature of the flow equations (so time-dependent equations) and in the nature of the inlet velocity who was made to vary in time in a manner representative to the Bay of Fundy flows, the same validated turbine geometry presented in Section 3.1 was used, applying the same turbulence model physics (SST) and using a similar mesh.

3.3.1 Boundary Conditions

The domain boundary conditions are provided in Table 4. At the inlet (z = -2D), a time- and depth-dependent velocity was imposed where the synthetic data was based on ADCP velocity measurements that were obtained in 2013 at the northern end of Grand Passage, Nova Scotia [28]. The conditions represent a typical flood tide when the mid-depth velocity ranged from 1.8 to 2 m/s.

The total velocity at the inlet was expressed as:

$$V(Y,t) = \bar{V}(Y) + v'(t) \tag{4}$$

where $\bar{V}(Y)$ is the mean velocity profile and $v'(t)$ is the turbulent component.

Table 4 Boundary Conditions

Boundary	Condition
Inlet	Unsteady Flow with an Averaged Normal Velocity $\bar{V}$= 2.05 m/s
Outlet	P_{rel} = 0 Pa
Tank Walls	No-Slip, Side Wall Velocity = 2.05 m/s Top Surface as a Free Surface
Turbine Walls	No-Slip
Domain Interfaces	Transient Rotor

The mean velocity profile was generated from the law-of-the wall which is given by:

$$\bar{V}(Y) = \frac{v_*}{\kappa}\ln\left(\frac{Y}{Y_0}\right) \tag{5}$$

where $\kappa = 0.4$ is the von Karman constant, v_* is the friction velocity and Y_0 is the bottom roughness lengthscale. The v_* and Y_0 parameters are based on the best fit to the ADCP data and are given by v_* = 0.0939 m/s and Y_0 = 0.0037 m. The resulting velocity profile is shown in Fig. 10.

Because an ADCP cannot measure v' directly, the measured dissipation rate of ε = 8.6 × 10^{-5} W/kg was used to obtain a realistic turbulent velocity [28]. A synthetic time series was generated by superimposing waves of random phase at wavenumbers below the Kolmogorov microscale, where the amplitude of each Fourier component was such that the theoretical form of the spectral density, S, was ensured, *i.e.* $S \sim k^{-5/3}$. In reality, ε and hence v' varies with depth; however, for this study, v' is taken independent of Y. The 20 second synthetic time series of v' is plotted in Fig. 11 a).

No-slip conditions were applied to every surface in the model, except the top water surface which was simulated as a free surface. The side walls of the simulation domain were given the same average velocity as the inlet flow to limit the impact of the wall on flow dynamics. The rotational rate of the cylindrical domain was set to achieve the desired tip speed ratio (TSR)

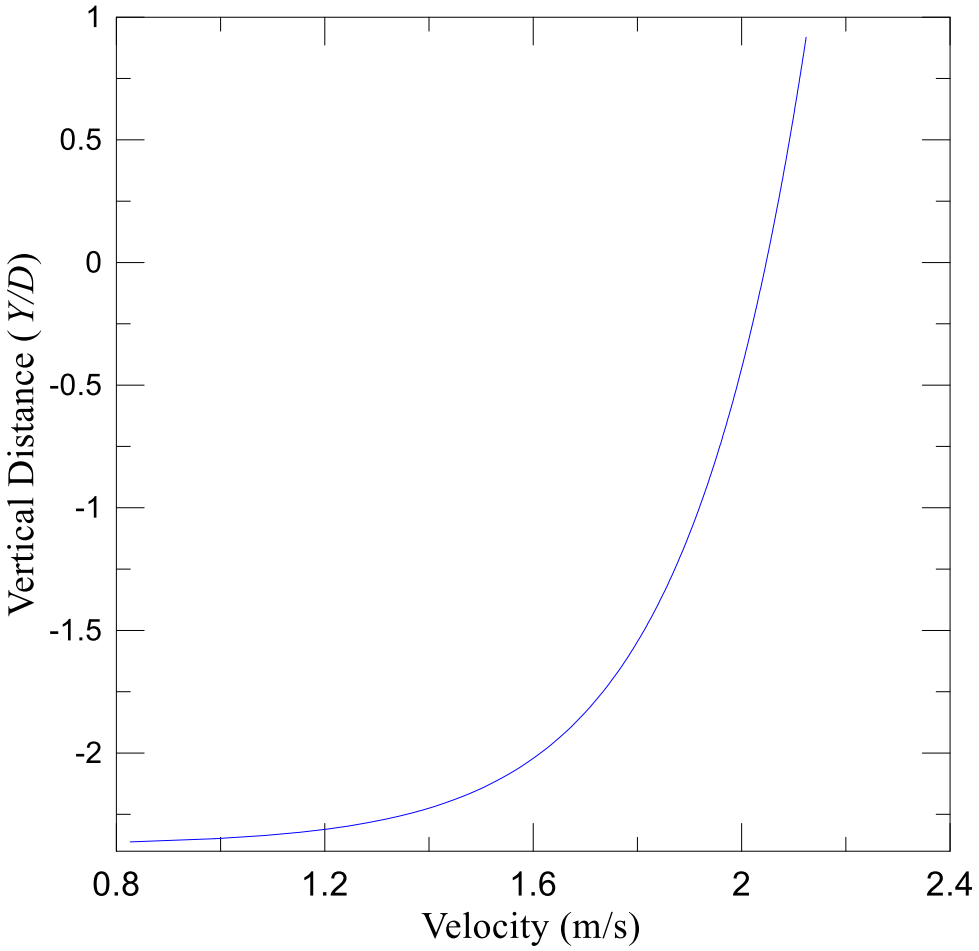

Figure 10 Mean velocity profile $\overline{V}$ as a function of *Y*.

In addition, steady state simulations were performed in order to enable the comparison of the wake behaviour. These simulations used only the constant mean velocity profile $\overline{V}(Y)$ as inlet velocity. Two thousand iterations were necessary to reach convergence in the wake.

In these steady simulations, the frozen-rotor quasi-steady approach was used to model the dynamics of the flow. Whereas fully transient-rotor simulations were used for the transient runs. With the exception of the inlet velocity and the frozen- or transient-rotor approach, all the simulations were performed with the same mesh and boundary conditions. All simulations are performed at constant TSRs.

Finally, all simulations were performed using between 26 and 30 cores on a Dell Precision T7810, 16 cores (2.4 GHz) hyper threaded with 128 GB of RAM. The computation time varied between 1 hour and 48hours (transient simulations) per simulation.

4 Results

4.1 Performance Calculations

Power and thrust coefficients are used for comparison was presented in Section 3.1. Because a velocity profile is used at the inflow, velocity varies with depth. Depending on the choice of reference velocity made (mean velocity profile $\bar{V}$ averaged on a swept area, velocity $\bar{V}(Y)$ at a specific location Y_1, etc.), power and thrust coefficients values can differ substantially. As shown by Fleming *et al.,* the power curve may be misrepresented if an incorrect reference velocity is taken [29]. They showed that the correct reference velocity is the one equal to the integral of the velocity over the rotor swept area. Thus, for all thrust and power coefficients computed in this paper, $V_A(t)$ is defined as the integral of the velocity over the rotor swept area.

For the unsteady simulations, total velocity $V_A(t)$ is defined by:

$$V_A(t) = v'(t) + \overline{V_A} \tag{6}$$

Therefore $V_A(t)$ is given at time t_1. Due to the advection time of the fluid from the inlet to the turbine, the inflow velocity at t_1 does not correspond to the fluid's velocity going through the turbine at t_1. To determine the actual velocity at the turbine, a time offset has been added. This offset is equal to the advection time of the fluid from the inlet to the turbine equal to 0.75 s.

Figures 11 a), b) and c) show, respectively, the evolution of V, C_p and C_t with time. In these figures, TSR is equal to 4 and the average velocity is set to 2.05 m/s. Twenty seconds of 'real data' were used to perform these simulations.

The magnitude of the fluctuations in the C_t is far higher than for C_p: C_p values varying from 0.24 to 0.4 whereas C_t values from 0.08 to 0.95. This large variation in the C_t values (consequently, also in blade loading) could lead to an increase of the turbine/blade fatigue and stress, possibly reducing the life expectancy of the device.

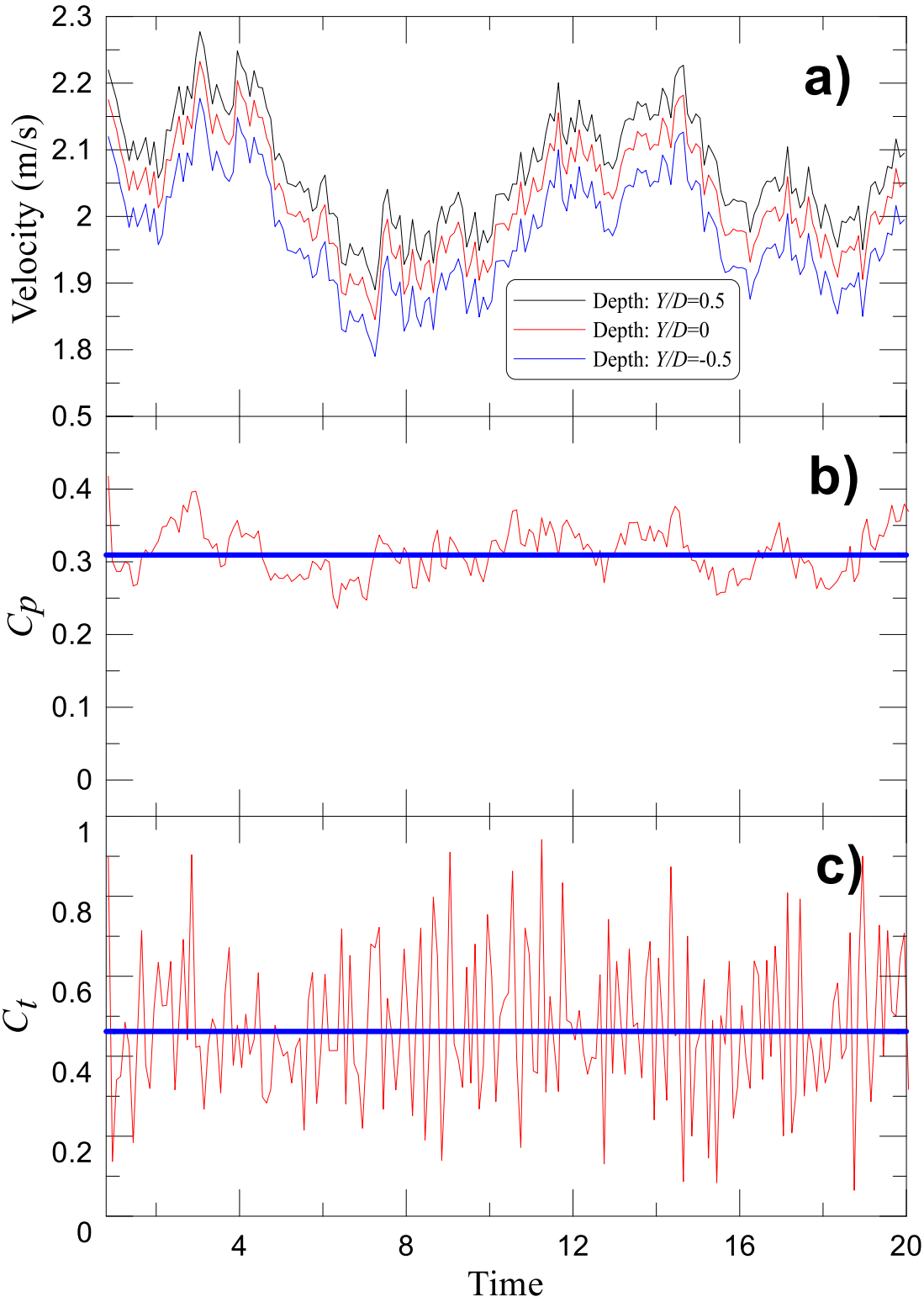

Figure 11 a) Inlet Velocity as a function of time for 3 different depths: *Y/D* = 0.5, *Y/D* = 0 and *Y/D* = -0.5 (*Y/D* = 0 corresponds to the hub height) b) C_p, as a function of time and c) C_t as a function of time (blue: coefficient from the steady simulation, red from the transient one).

4.2 Power and Thrust Coefficients

With the inlet velocity being time-dependent in the transient simulations, the instantaneous velocity varies from 1.75 to 2.2 m/s (when the average velocity is 2.05 m/s). Therefore, for comparison, it was decided to perform the steady simulations with the same range of input speeds. Results in Fig. 12 include the results of steady simulations covering a range of tip speed ratios (TSR = 3 – 4.5) and velocities (1.75-2.2 m/s). Transient simulations cover a range of TSR (3 - 4.5) obtained for one transient inlet velocity having an average of 2.05 m/s. Figure 12 shows the comparative C_p-TSR and C_t-TSR curves for steady and unsteady flow.

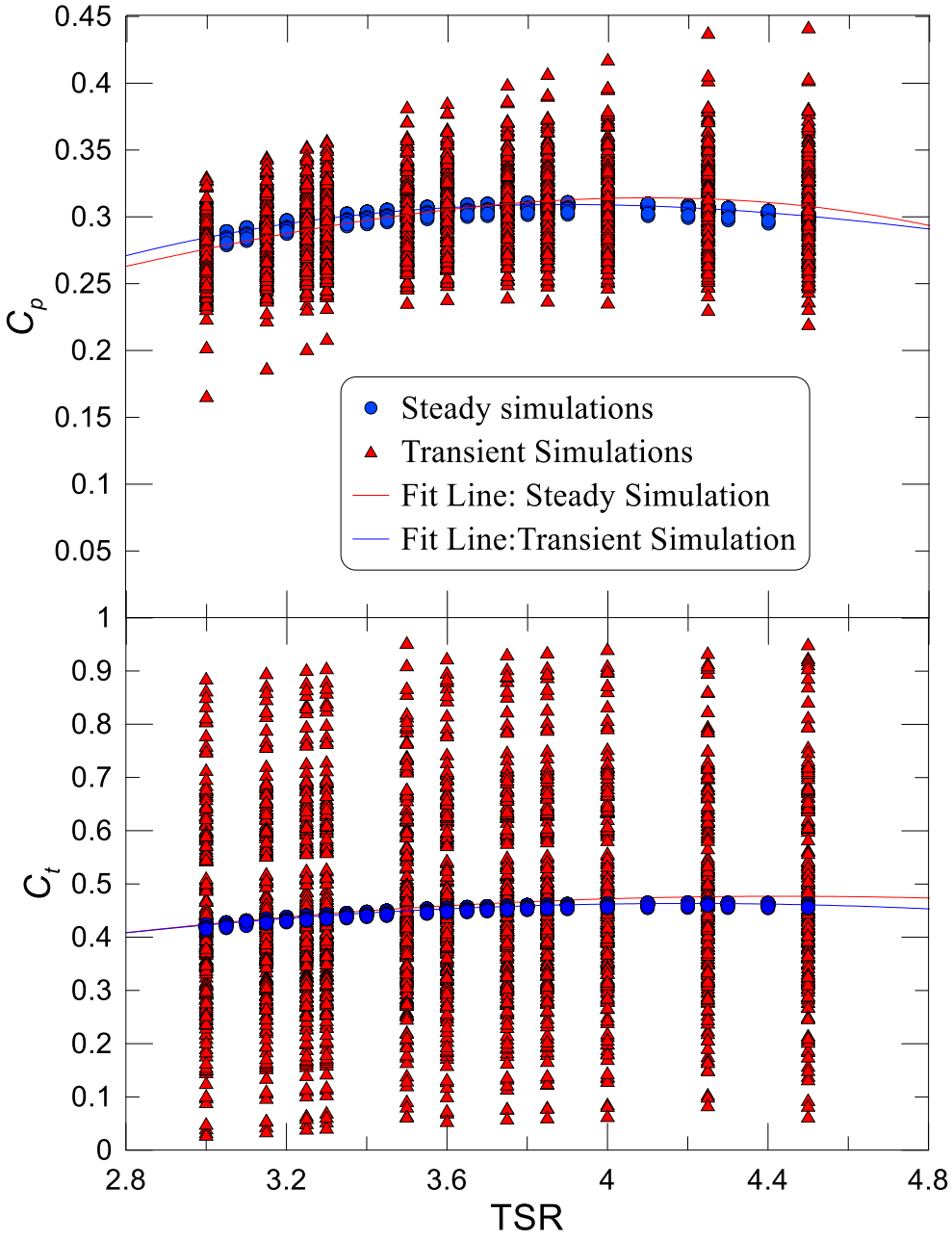

Figure 12 C_p and C_t as a function of TSR.

Both C_p and C_t follow a similar trend for steady and unsteady simulations. However, in the transient results, the fluctuation amplitude in the C_p and C_t values is much higher than for steady flow results.

The turbine's overall performance for an unsteady flow is comparable to the one obtained for a steady flow. The steady flow C_p curve has an average relative difference of 0.83% and average absolute difference of 0.003 below unsteady simulations values. Likewise, the predicted C_t curve has an average relative difference of 0.07% below unsteady simulations values. As can be seen, the relative difference grows with TSR to reach 0.5% for TSR=4.5.

4.3 Mechanical Performance

Following the presentation of results from Dr. Bjorn Elsaesser's group experiments [1], the mechanical performance of the turbine was assessed. To do so, new simulations were run with changed inlet conditions. Steady simulations covering a wider range of velocities (1.45 to 2.3 m/s) were performed at constant TSRs (3, 3.5 or 4), whereas in the transient simulations, three different velocities (integral of the velocity on the rotor swept area) were used: 1.6, 1.8 and 2.05 m/s. TSR remained constant for the duration of a simulation. The comparison of the mechanical power against inflow velocity for these three TSR-values is shown in Fig. 13.

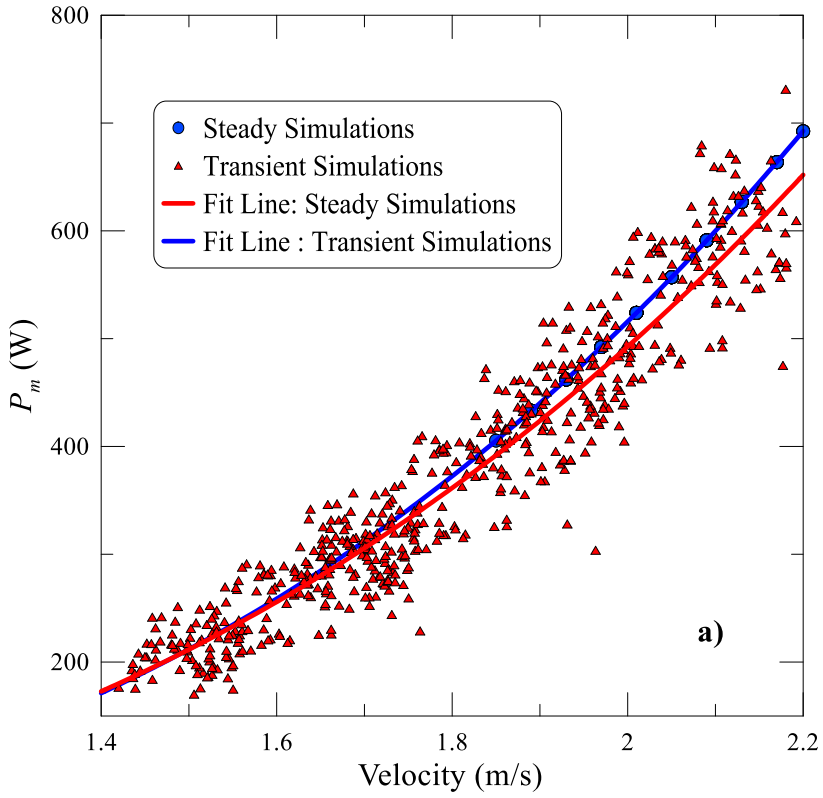

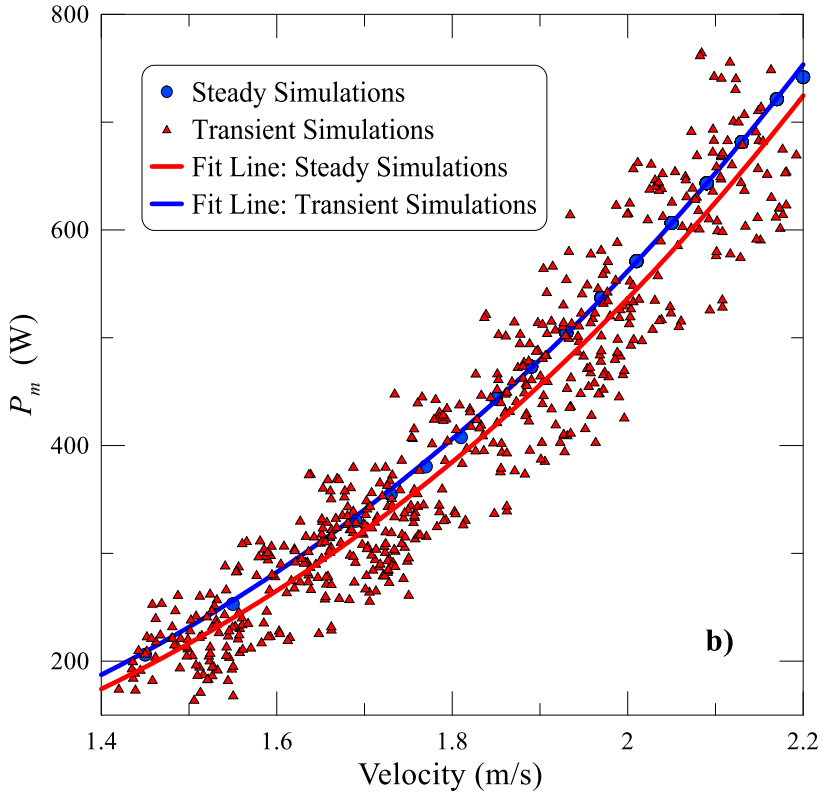

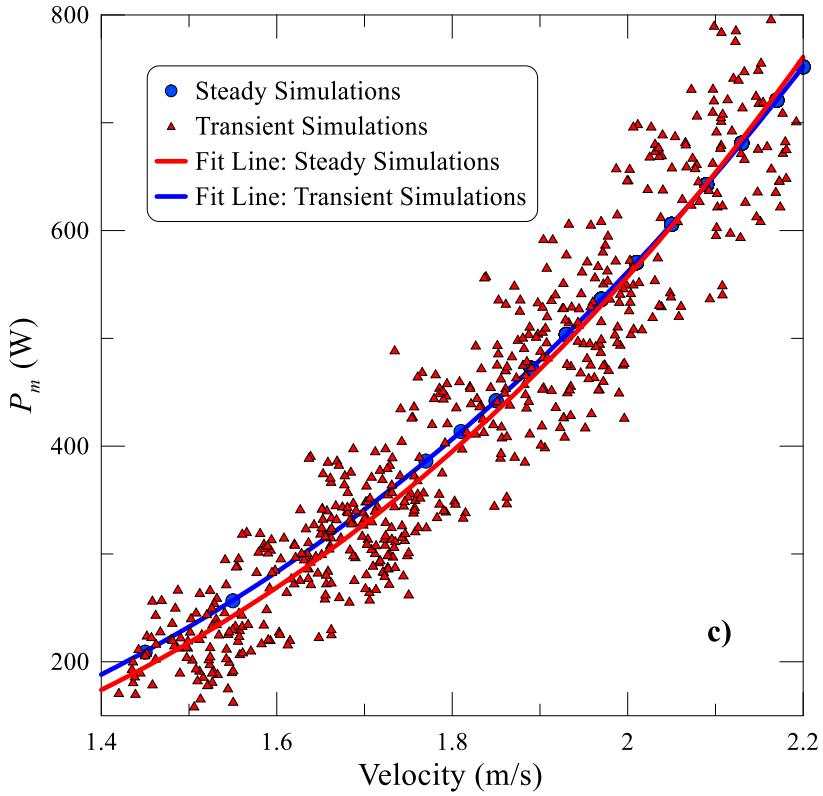

Figure 13 8 Steady and transient mechanical power against inflow velocity for: a) TSR = 3, b) TSR = 3.5 and c) TSR = 4.

In each case, the relationship between the mechanical power P_m and the velocity follows the power law expected from Eq. (3). The mechanical power is proportional to the power in the flow and thus the cube of the inflow velocity. The relationship is very consistent for the steady and unsteady flow even if the amount of scatter in the instantaneous P_m values is important for transient results.

Taking a closer look at the curves for each TSR, for TSR = 3.5, the unsteady tests mechanical performance is always lower than the steady one: approximately 7 W (3.3%) less than the steady tests at 1.45 m/s and 27.7 W (3.3%) less than the steady tests at 2.3 m/s. For TSR = 3 or 4, the difference between the steady and the transient mechanical performance depends on the velocity-value. For TSR = 3, the difference is close to 0 at 1.45 m/s and equal to 50 W (6.3%) and the opposite trend is seen for TSR = 4.

4.4 Wake Characteristics

Velocity deficit and turbulence intensity were computed in order to visualize what is happening in the wake, and are defined as:

$$V_{deficit} = 1 - \frac{V_W}{\bar{V}_A} \tag{7}$$

$$TI = \frac{100}{\bar{V}_A}\sqrt{\frac{2}{3}k} \tag{8}$$

where V_W is the local wake velocity and k is the turbulent kinetic energy. $\bar{V}_A$ is the time average of the integral of the velocity over the rotor swept area and therefore remains constant for the duration of the simulation (so no time offset was added to consider the advection time from the inlet to the turbine even for transient simulations).

To visualize clearly what is happening in the wake, dimensionless velocity (V/V_0) are plotted in Fig. 14 at different locations along the wake, both for steady and transient simulations. Because in transient simulations, the wake is constantly evolving, results only for a single specific time value are presented. This was chosen to be 20 s because it is a good compromise between the time needed to obtain a fully developed wake which can be observed to take approximately 10 s, and a simulation which lasts for too long.

The shape of velocity profile through the wake is different: a cylindrical-shaped wake for transient flow whereas there is a “turbine-shaped” wake for steady simulations. Moreover, the velocity deficit seems to disappear faster in the constant velocity simulations. Figure 14 a), b), c) and d) also illustrates the effects, of the fixed rotor blades in the steady simulation. In contrast, in transient simulations, with the Transient Rotor approach, the blades are always moving. That is why a large circle profile can observe in the transient simulation.

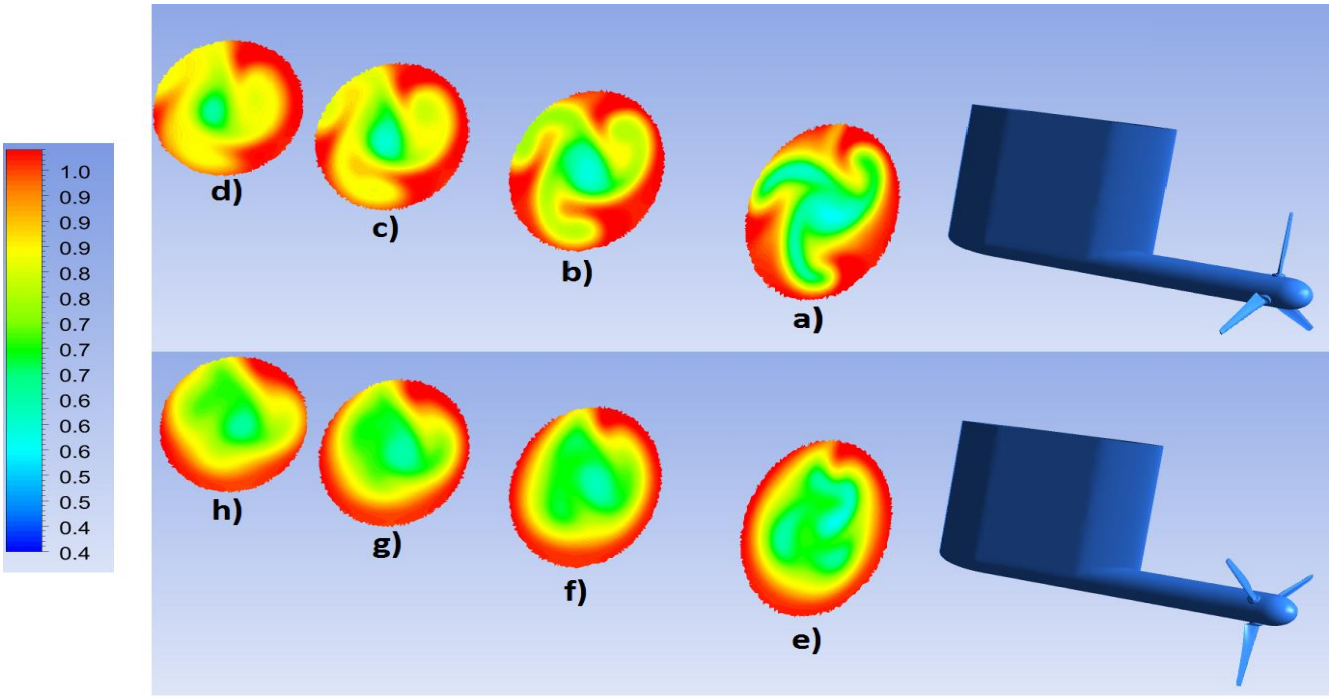

Figure 14 Normalized velocity V/V_0 for steady simulations at a) 3*D*, b) 5*D*, c) 7*D* and d) 9*D* and transient simulations at e) 3*D*, f) 5*D*, g) 7*D* and h) 9*D*.

Figure 15 represents the normalized velocity on mid-vertical plane. It shows that the velocity deficit is more important for transient simulations in the far field wake (7*D* and 9*D*) but it is the opposite in the near field. As mentioned earlier, depending on the type of inflow velocity used, the shape of the wake is different. The wake is wider for the transient simulation and disappears more slowly. At a distance of 10*D*, velocity is approaching the inflow velocity for steady state whereas the velocity deficit is still important in the second case. Even at a distance of 20*D*, the flow is still affected by the turbine in the transient case.

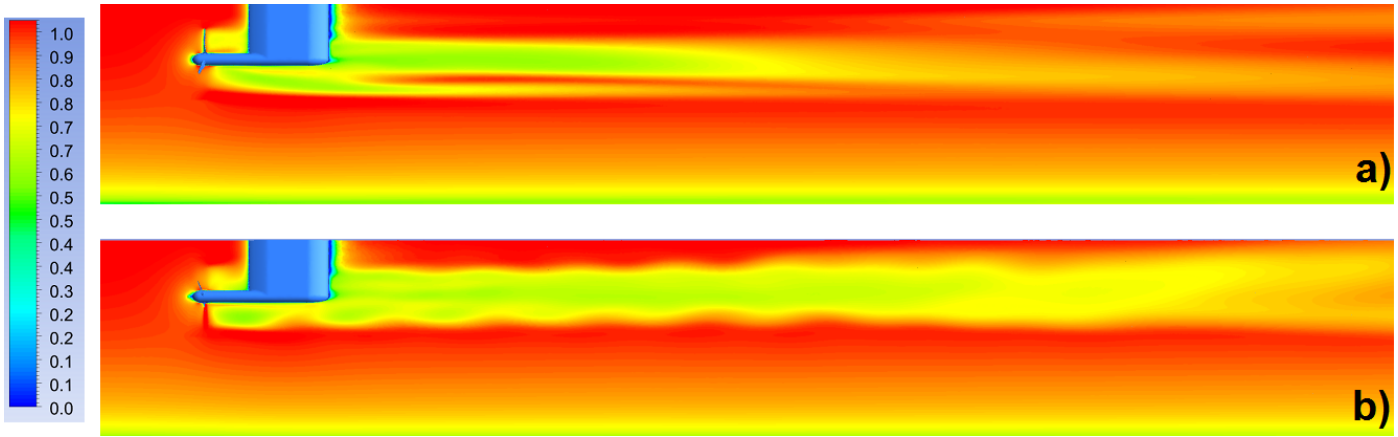

Figure 15 Normalized Velocity V/V_0 on mid-vertical plane for a) steady flow, b) transient flow at *t* = 20 s.

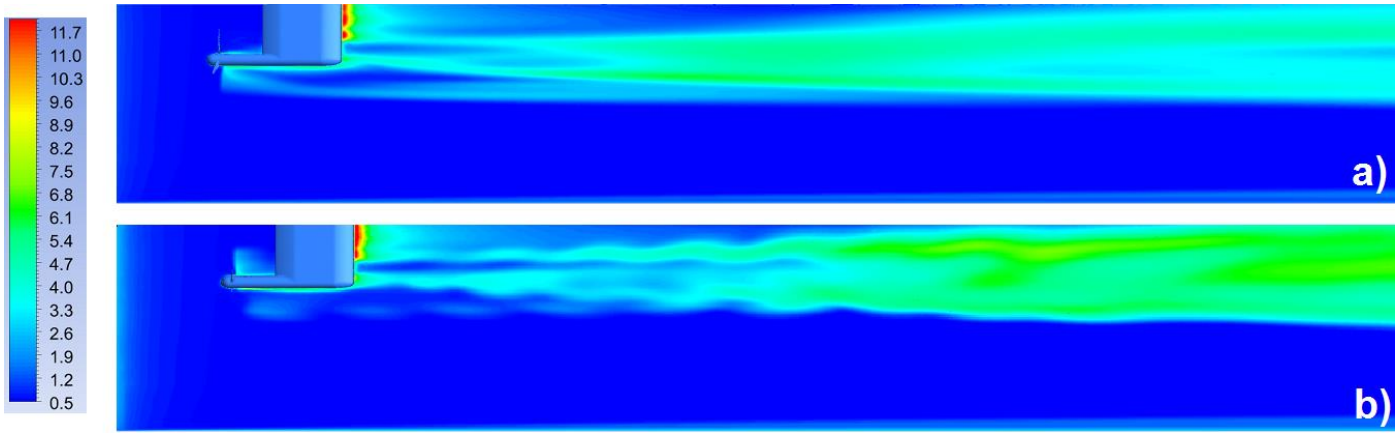

Figure 16 Turbulence intensity on mid-vertical plane for a) steady flow, b) transient flow at *t* = 20 s.

Figure 16 presents the turbulence intensity along the centre plane of the wake. Unlike velocity profiles, turbulence intensity profiles are much the same in both cases: turbulence is still significant at a distance of 20*D* and increases as moving away from the turbine. When turbulence intensity is lower than 4% in the near wake, it is approximately 6% at a distance of 20*D*. As above, turbulence is higher in the transient case, especially in the far wake: at a distance of 20*D*, maximum turbulence intensity is 3.6% for constant flow simulations and 5.7% for the unsteady simulation. This may due to the large fluctuation of the inlet velocity during the simulation.

Figures 17 and 18 present the values of turbulence intensity and velocity deficit over horizontal lines and vertical lines at 5*D*, 10*D*, 15*D* and 20*D*. First, both for velocity deficit and turbulence intensity, there is no symmetry along *Z*. In steady simulation, this is due to the Frozen Rotor approach which forces the fluid to twist around the blades. That twist is always generated in the same side of the blade and thus it creates a deflection at *X/D*= -0.5 as seen in Figs. 17 and 18 b)-c)-d). At 5*D*, irregularities in the turbulence intensity can be observed at *x/D* = 0 and ± 0.5 (especially in the transient simulations). These irregularities correspond to the turbulence due to root and tip losses, and nacelle structure interaction.

Regarding the velocity deficit, the wake seems to become wider from 5*D* to 20*D*, both in the horizontal and vertical directions. The velocity deficit is not confined anymore between -0.5 and 0.5 m (in both directions at 5*D*) but between -0.75 and 0.9 m (vertical direction at 20*D*). The results demonstrate also that average velocity deficit is higher in the transient simulations than steady simulations and so the velocity deficit disappears faster in the constant velocity simulations. For example, the average velocity deficit is approximately 0.09 at a horizontal distance of 10*D* for a constant velocity inflow and 0.15 for transient simulations. However, velocity deficit in constant velocity simulations seems to be over-predicted outside of the wake.

Regarding turbulent intensity, results may be difficult to interpret: for turbulence intensity as a function of vertical distance, turbulence is higher for transient results than steady one. For instance, at a distance of 15*D*, average turbulence intensity is approximately 3% for steady state simulations and 4% for transient. However, it is not so obvious when looking to turbulence as a function of horizontal distance *e.g.* at a distance of 20*D*, average turbulence intensity is equal to 1.7% for transient flow and 1.9% for steady flow simulations. It can also be seen that turbulence increases from 5*D* to 20*D* in both directions.

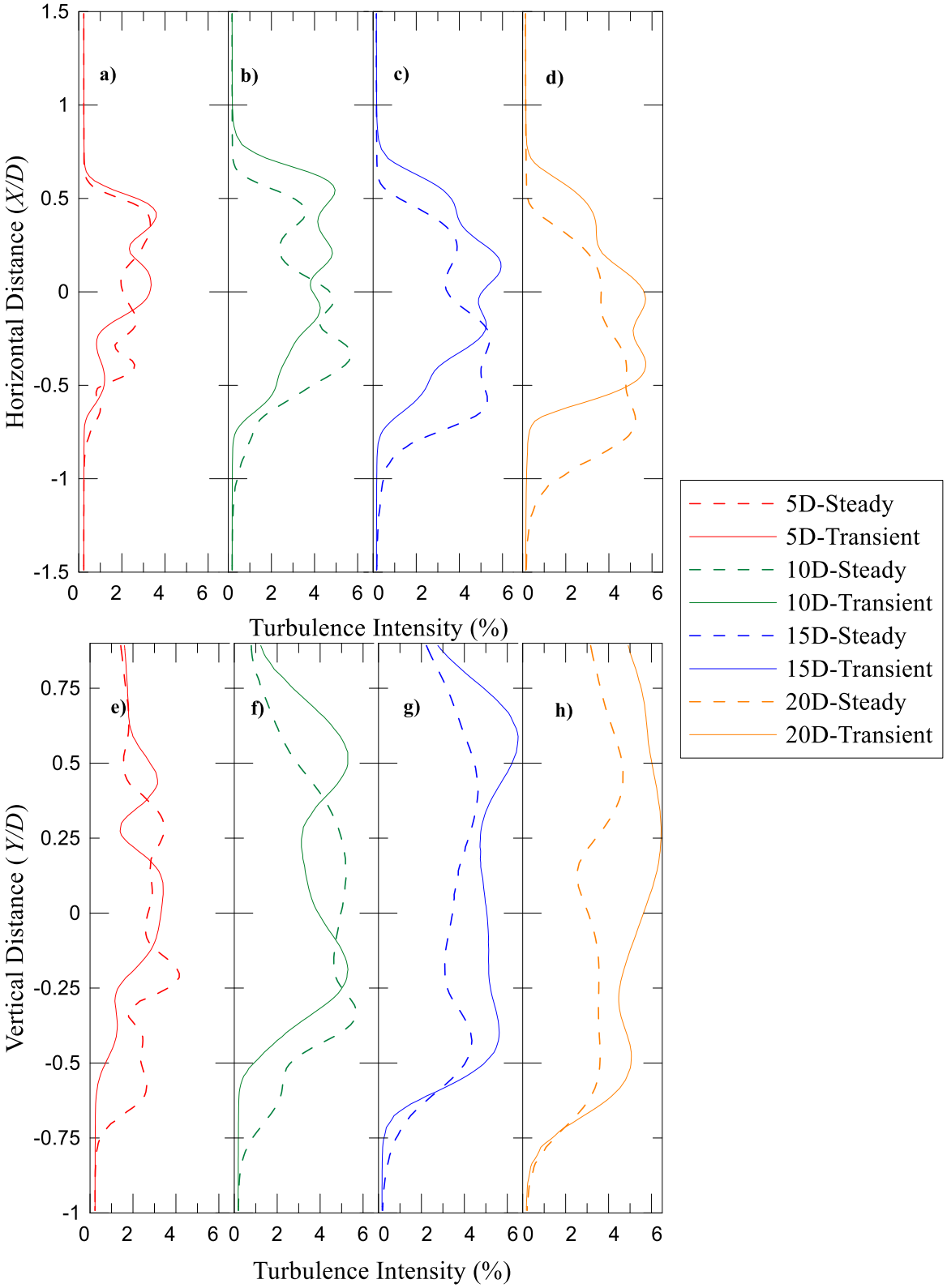

Figure 17 Turbulence intensity: a) Horizontal - 5*D*, b) Horizontal - 10*D*, c) Horizontal - 15*D*, d) Horizontal - 20*D*, e) Vertical - 5*D*, f) Vertical - 10*D*, g) Vertical - 15*D*, h) Vertical - 20*D*.

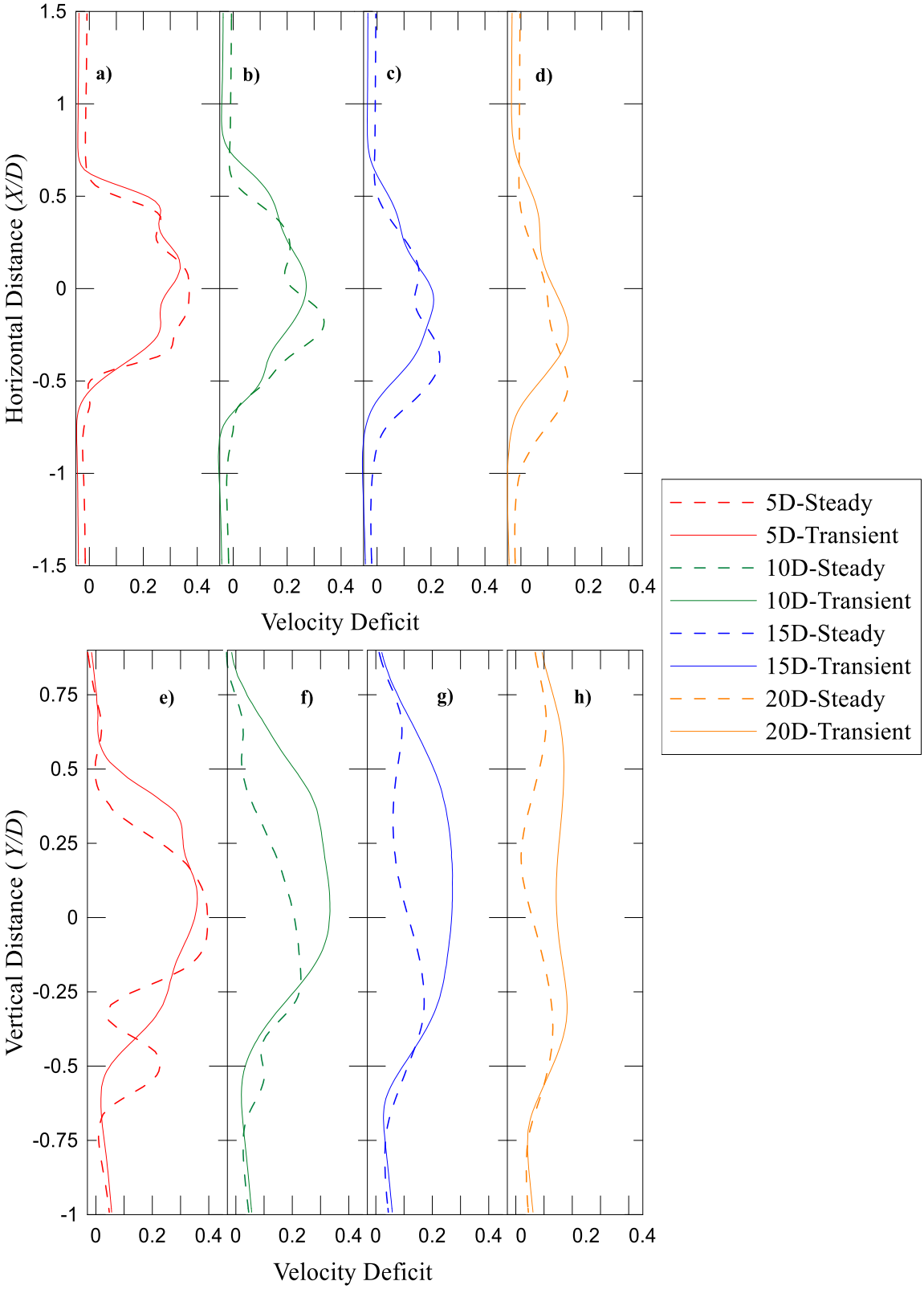

Figure 18 Velocity deficit: a) Horizontal - 5*D*, b) Horizontal - 10*D*, c) Horizontal - 15*D*, d) Horizontal - 20*D*, e) Vertical - 5*D*, f) Vertical - 10*D*, g) Vertical - 15*D*, h) Vertical - 20*D*.

4.5 Conclusions

A numerical model of a three bladed horizontal axis tidal turbine under realistic turbulent tidal flow has been created. The preliminary results of this investigation have been compared with steady flow numerical model results with good agreement in trends. Prediction of both C_p and C_t are very similar in both cases. These similar trends observed in both C_p and C_t curve are important as they indicate that the appropriate flow physics are being accounted for. Only TSR values related to maximum C_p and C_t changed. For C_p curves, tip speed ratio is approximately equal to 3.9 in steady flow and 4.1 for transient conditions. In transient flows, this results however in an approximate 4% reduction in performance (for TSR = 3.5), though there is increased uncertainty due to the levels of scatter in the numerical data points.

Velocity deficit plots show the wake is wider in transient simulations than steady ones. The velocity deficit disappears also faster in the constant velocity simulations. Turbulent effects in the wake seem to increase after a distance of 10D downstream of the turbine in this setup, as shown in Fig. 13. These turbulence effects are higher in the transient simulations.

This comparative analysis of numerical steady and transient simulations shows the impact of the unsteadiness of realistic tidal flows on the performance of tidal turbines. In view of the above, the current use of steady state testing (numerical or experimental) for design stage can be questioned. The observed changes in the wake's characteristics and the high variations of the loads on the blades (reference to Ct-curve as a function of time) must also be better assessed.

5 Dissemination and Technology Transfer

For this project, performed over a 6-month period, one conference paper was submitted to the 3rd Asian Wave and Tidal Energy Conference (AWTEC), provided in Appendix A. From discussion between Drs. Hay and Groulx, the quality and quantity of work performed through this project is of a very high level that a full length journal paper based on the work and presenting additional results beyond the AWTEC paper will be prepared and submitted to the International Journal of Marine Energy; this paper will be provided to OERA when published.

Additionally, during the ramp up period of the work, while Mr. Leroux was learning to apply the CFX methodology created previously at the LAMTE, the numerical studies that were performed at that point, simulating, and validating, turbine performance based on a geometry and data from IFREMER in France, proved to be very accurate and interesting. Therefore, the results of this early work will be presented at the Australian Ocean Renewable Energy Symposium (AORES) in Melbourne next October. The abstract for that work is presented in Appendix B. The symposium will be inviting full papers to be submitted to the International Journal of Marine Energy after the meeting; we hope to submit such a paper at this point.

The capability and demonstration of using real tidal flow turbulent data, taken directly from the Bay of Fundy, in order to study the turbine and wake behaviour in a real environment represents an important advance in numerical capability for the researchers at Dalhousie University. This also greatly enhance the track record of the researchers (abstracts, posters and papers) in the specific Tidal power area.

6 Publications

One conference paper was directly prepared and submitted out of this work:

LEROUX, T., OSBOURNE, N., McMILLAN, J.M., GROULX, D., HAY, A.E. (2016) *Numerical Modelling of a Tidal Turbine Behaviour under Realistic Unsteady Tidal Flow*, Asian Wave and Tidal Energy Conference Series (AWTEC), Singapore, 10 p. – accepter and to be presented in October 2016

One journal paper expending on this work will also be written and submitted to the International Journal of Marine Energy.

As mentioned in the previous section, an abstract was also submitted and work will be presented in Melbourne, Australia, also in October 2016:

LEROUX, T., OSBOURNE, N., GROULX, D. (2016) *Numerical Study into an Horizontal Tidal Turbine Wake Velocity Deficit – IFREMER-LOMC Turbine*, Australian Ocean Renewable Symposium, Melbourne (Australia) – to be presented in October 2016

Out of this symposium, journal papers will be invited for publication in International Journal of Marine Energy.

7 Expenditure of OERA Funds

Removed, this copy

8 Employment Summary

Five researchers have been involved on this project as shown on Table 6.

Table 5 Employment Summary

Name	Position	Student	Scientific Contribution	Duration on Project
Tanguy Leroux (Full Time)	Undergraduate Research Engineer	Yes (UG)	- Performs numerical modeling and research - Result analysis and presentation - Abstract and paper writing	Jan. 2016 to July 2016
Nicholas Osbourne (Part Time)	Research Engineer	No	- Assist in numerical modeling and research - Result analysis - Abstract and paper review	
Justine McMillan (Part Time)	PhD Student	Yes (PhD)	- Provided Bay of Fundy turbulent velocity data - Abstract and paper review	

Dr. Alex E. Hay **(Part time – no salary from grant)**	Professor	No	- Supervision of real-tidal turbulent velocity data work - Abstract and paper review	
Dr. Dominic Groulx **(Full time – no salary from grant)**	Associate Professor	No	- Principal investigator and research surpervisor - Abstract and paper writing	

9 Conclusions and Recommendations

9.1 Conclusions

Three dimensional transient simulations where perform to study the flow around, and the tidal turbine, behaviour under fully transient, turbulent conditions, including inlet conditions to the simulations that were transient and based on real Bay of Fundy turbulent velocity measurements. The turbine geometry used was a simple three-bladed horizontal axis tidal turbine (HATT) using blade designed by Dalhousie Engineering researchers based on NREL S814 wing profiles.

The numerical method used, using a steady-state frozen rotor physics, had already been validated by comparing the numerical results to experimental tow-tank tests that had been performed by Dalhousie Engineering researchers collaborating with colleagues at the University of Strathclyde.

Using the fully transient approach, the results of this project shows that on average the turbine behaved the same way when it comes to average power production and thrust loading (average C_p and C_t). However, under true transient inlet conditions, the amount of power produces and thrust on the turbine blades was greatly time-dependent, with the thrust sometime being completely absent, while doubling from the average value at other times. Directly related to the problematic identified by the Queen's University group, it appears, that even through power production is constantly varying under real transient conditions, the overall amount of power produce by the turbine would average out to the same value predicted using constant velocity and steady-state studies. This result is interesting, comforting, but should be taken with a grain of salt until more experimental tests are carried out in real-tidal environment.

When it comes to the wake, it is clear that the wake calculated using the fully transient method provides a more accurate representation of a real wake compared to the steady-state studies. The transient simulations predict a wake that is more physical, that endures on a longer distance and that is wider than the steady-state prediction. This point to the fact that transient studies should be used for true wake numerical characterization.

Looking specifically at the three objectives defined in section 2, the following has been done so far:

1. The numerical method was adapted and the first simulations using representative Bay of Fundy velocity data were performed;
2. A proper study of the wake was done, where it was found that transient wake are larger and longer than those predicted before using other methods;
3. Comparison between transient and steady-state turbine performance, and wake behaviour, has been done.

9.2 Recommendations

From this work, the following recommendations can be made:

- ✓ Analysis of the large amount of data will be continued by Dr. Groulx in the future, with interesting and meaningful additional conclusions to be communicated through conference and journal publications;

- ✓ In the future, longer and larger simulations should be performed. Longer in the sense that 20 s simulations were extremely useful for this shorter term project; however, simulations for a few minutes of flow (which will take a week or two of simulation) would provide greater perspective in the overall turbine and wake dynamics. Larger when it comes to the length of the wake for this system; currently the wake persists beyond the 20*D* downstream length in the simulation. It is not clear yet how long a turbine wake would be, so pushing the size of the simulated volume would be something enlightening;

- ✓ Various inlet conditions, at different level of turbulence (also taken from the Bay of Fundy) should now be used in order to determine their impact on wake and turbine behaviour;

- ✓ Now that a better wake is resolved, the next step in this overall wake study could be taken, now looking at the impact of the wake from a first turbine impacting the performance and behaviour of a second turbine downstream, while varying the distance between the turbines. This next series of work will start to put this entire framework in the context of tidal turbine arrays.

- ✓ Finally, with developers about to start installing their device in the Bay of Fundy, it would be time to have a concerted effort between the developers, FORCE, experimental wake characterization researchers (oceanographers) and tidal fluid engineering researchers to look, measure, characterize and simulate (validate) the wake from the various devices, interacting with the Bay of Fundy, and amongst themselves. Studies should be performed experimentally in the near- and far-field, numerically at large Bay of Fundy (or fraction of Bay) scales using the best available tools to simulate oceanic flows and turbines (actuator disks or other) and at smaller turbine scales using fully transient and turbulent to fully resolve the near-field and provide information about the far-field wake from a truly rotating turbine similar to the various developers' turbines.

References

1. JEFFCOATE, P., ELSAESSER, B., WHITTAKER, T., BOAKE, C. (**2014**) *Testing Tidal Turbines - Part 1: Steady Towing Tests vs. Tidal Mooring Tests*, International Conference on Offshore Renewable Energy, Glasgow (Scotland), 9 p.
2. OSBOURNE, N. (**2015**) *3D Modelling of a Tidal Turbine - A Numerical Investigation of Wake Phenomena*, in *Mechanical Engineering*2015, Dalhousie University: Halifax, NS. 130 p.
3. OSBOURNE, N., GROULX, D., PENESIS, I. (**2015**) *3D Modelling of a Tidal Turbine - An Investigation of Wake Phenomena*, The 11th European Wave and TIdal Energy Conference (EWTEC), Nantes (France), 10 p.
4. MCMILLAN, J., HAY, A., KARSTEN, R., TROWSE, G. (**2013**) *Comprehensive Tidal Energy Resource Assessment in the lower Bay of Fundy, Canada*, The 10th European Wave and Tidal Energy Conference, Aalborg, Denmark, 10 p.
5. MCMILLAN, J.M., HAY, A.E., LUECK, R.G., WOLK, F. (**2015**) *An Assessment of the Dissipation Rates at a Tidal Energy Sites using a VMP and an ADCP*, 11th European Wave and Tidal Energy Conference, Nantes (France), 8 p.
6. MCNAUGHTON, J., HARPER, S., SINCLAIR, R., SELLAR, B. (**2015**) *Measuring and Modeling the Power Curve of a Commercial-Scale Tidal Turbine*, 11th European Wave and Tidal Energy Conference, Nantes (France), 9 p.
7. BAHAJ, A.S., MOLLAND, A.F., CHAPLIN, J.R., BATTEN, W.M.J. (**2007**) *Power and thrust measurements of marine current turbines under various hydrodynamic flow conditions in a cavitation tunnel and a towing tank,* Renewable Energy, v.32, p.407-426.
8. DOMAN, D.A., MURRAY, R.E., PEGG, M.J., GRACIE, K., JOHNSTONE, C.M., NEVALAINEN, T. (**2015**) *Tow-tank testing of a 1/20th scale horizontal axis tidal turbine with uncertainty analysis,* International Journal of Marine Energy, v.11, p.105-119.
9. MYCEK, P., GAURIER, B., GERMAIN, G., PINON, G., RIVOALEN, E. (**2014**) *Experimental study of the turbulence intensity effects on marine current turbines behaviour. Part I: One single turbine,* Renewable Energy, v.66, p.729-746.
10. BATTEN, W.M.J., BAHAJ, A.S., MOLLAND, A.F., CHAPLIN, J.R. (**2008**) *The prediction of the hydrodynamic performance of marine current turbines,* Renewable Energy, v.33, p.1085-1096.
11. BAHAJ, A.S., BATTEN, W.M.J., MCCANN, G. (**2007**) *Experimental verifications of numerical predictions for the hyrodynamic performance of horizontal axis marine current turbines,* Renewable Energy, v.32, p.2479-2490.
12. HARRISON, M.E., BATTEN, W.M.J., MYERS, L.E., BAHAJ, A.S. (**2009**) *A comparison between CFD simulations and experiments for predicting the far wake of horizontal axis tidal turbines*, The 8th European Wave and Tidal Energy Conference, Uppsala, Sweden, 10 p.
13. JO, C.H., LEE, J.H., RHO, Y.H., LEE, K.H. (**2014**) *Performance analysis of a HAT tidal current turbine and wake flow characteristics,* Renewable Energy, v.65, p.175-182.
14. MULLER, P., SAINCLAIR, F., CARLISLE, A., DELAFOSSE, C. (**2015**) *Tidal Current Turbine Optimization using CFD Simulation*, 11th European Wave and Tidal Energy Conference, Nantes (France), 7 p.
15. STARZMANN, R., JEFFCOATE, P., SCHOLL, S., BISHOF, S., ELSAESSER, B. (**2015**) *Field Testing a full-scale Tidal Turbine - Part 1: Power Performance Assessment*, 11th European Wave and Tidal Energy Conference, Nantes (France), 7 p.
16. LEE, J.H., PARK, S., KIM, D.H., RHEE, S.H., KIM, M.-C. (**2012**) *Computational methods for performance analysis of horizontal axis tidal stream turbines,* Applied Energy, v.98, p.512-523.

17. O'DOHERTY, T., MASON-JONES, A., O'DOHERTY, D.M., BYRNE, C.B., OWEN, I., WANG, Y.X. (**2009**) *Experimental and Computational Analysis of a Model Horizontal Axis Tidal Turbine*, The 8th European Wave and Tidal Energy Conference, Uppsala, Sweden, p. 833-841.
18. MCSHERRY, R., GRIMWADE, J., JONES, I., MATHIAS, S., WELLS, A., MATEUS, A. (**2011**) *3D CFD modelling of tidal turbine performance with validation against laboratory experiments*, The 9th European Wave and Tidal Energy Conference, Southampton, UK, 7 p.
19. AHMED, U., AFGAN, I., APSLEY, D.D., STALLARD, T., STANSBY, P.K. (**2015**) *CFD Simulations of a Full-Scale Tidal Turbine: Comparison of LES and RANS with Field Data*, 11th European Wave and Tidal Energy Conference, Nantes (France), 8 p.
20. WANG, X., DAY, A.H. (**2015**) *CFD Turbulence Modelling of Tidal Turbine Unsteady Blade Load*, 11th European Wave and Tidal Energy Conference, Nantes (France), 10 p.
21. BLACKMORE, T., GAURIER, B., MYERS, L., GERMAIN, G., BAHAJ, A.S. (**2015**) *The Effect of Freestream Turbulence on Tidal Turbines*, 11th European Wave and Tidal Energy Conference, Nantes (France), 8 p.
22. MYCEK, P., GAURIER, B., GERMAIN, G., PINON, G., RIVOALEN, E. (**2014**) *Experimental study of the turbulence intensity effects on marine current turbines behaviour. Part II: Two interacting turbines,* Renewable Energy, v.68, p.876-892.
23. WILCOX, K.W., MCLEOD, I.M., GERBER, A.G., JEANS, T., CULINA, J. (**2015**) *Validation of High-Fidelity CFD Simulation of the Unsteady Turbulent TIdal Flow in Minas Passage*, 11th European Wave and Tidal Energy Conference, Nantes (France), 13 p.
24. HAY, A.E., MCMILLAN, J., CHEEL, R., SCHILLINGER, D. (**2013**) *Turbulence and Drag in a High Reynolds Number Tidal Passage targeted for In-stream Tidal Power*, IEEE Oceans'13, San Diego (USA)
25. CURRIE, G., OSBOURNE, N., GROULX, D. (**2016**) *Numerical Modelling of a Three-Bladed NREL S814 Tidal Turbine*, AWTEC 2016, Singapore, 10 p.
26. MENTER, F. (**1994**) *Two-equation eddy-viscosity turbulence models for engineering applications,* AIAA Journal, v.32, p.1598-1605.
27. GUO, Q., ZHOU, L.J., WANG, Z.W. (**2015**) *Numerical simulation of cavitation for a horizontal axis marine current turbine,* IOP Conference Series: Materials Science and Engineering, v.72, p.042045.
28. MCMILLAN, J.M., HAY, A.E., LUECK, R.G., WOLK, F. (**2016**) *Rates of Dissipation of Turbulent Kinetic Energy in a High Reynolds Number Tidal Channel,* Journal of Atmospheric and Oceanic Technology, v.33, p.817-837.
29. FLEMING, C.F., MCINTOSH, S.C., WILLDEN, R.H.J. (**2013**) *Tidal Turbine Performance in Sheared Flow*, EWTEC 2013, Aalborg, Denmark, 8 p.

Appendix A
AWTEC 2016 - Paper

Numerical Modelling of a Tidal Turbine Behaviour under Realistic Unsteady Tidal Flow

T. Leroux[#1], N. Osbourne[#2], J.M. McMillan[*3], D. Groulx[#4], A.E. Hay[*5]

[#]*Department of Mechanical Engineering, Dalhousie University*
Halifax, Nova Scotia, Canada

[1]tn876184@dal.ca

[2]nick.a.osbourne@dal.ca

[4]dominic.groulx@dal.ca

[*] *Department of Oceanography, Dalhousie University*

[3]justine.mcmillan@dal.ca

[5]alex.hay@dal.ca

Abstract— **This paper presents the results of three dimensional numerical simulations of a three-bladed horizontal axis tidal turbine (HATT) under realistic turbulent tidal flow conditions. All results provided incorporate the Reynolds-averaged Navier-Stokes (RANS) Shear Stress Transport (SST) turbulence model. Simulations cover a range of tip speed ratios (TSR = 3 – 4.5) and flow velocities (1.6, 1.8 and 2.05 m/s) at a fixed hub pitch angle of approximately 28°. Simulations are performed at a time-dependent, turbulent inflow velocity based on measurements obtained in Grand Passage, Nova Scotia. Thrust and power coefficients are compared to numerical results obtained in steady flow for validation purposes. The results show a good level of agreement between steady and transient simulations. Results of a power production comparison show a small reduction in power production (4%), when comparing turbine operation in a realistic unsteady tidal flow to operation in a steady flow. Near field and far field wake propagation is also investigated and compared to the wake obtained with a steady flow.**

Keywords— **Computational Fluid Dynamics (CFD), Horizontal Axis Tidal Turbine (HATT), Transient Simulations, Reynolds-averaged Navier-Stokes (RANS), Real Tidal Flow Inlet Conditions**

I. Introduction

General concerns of global warming, along with the cost of fossil fuels, are rising. As a consequence, increasing focus is put on the development of renewable energy industries. Some of these industries, such as hydroelectricity or on-shore wind, are well established. On the other hand, marine energy sources are not yet exploited.

Unlike on-shore wind industries, marine energy industries are facing new challenges due to the harsher conditions of the environment in which they operate. Oceans present their own physical challenges that make development, manufacturing and marine energy device maintenance difficult and costly. These challenges include: salinity, high turbulence levels, rapid tidal flow, environmental issues and poor accessibility. It is nevertheless believed that the outcome is worth the effort.

It has been estimated that tidal stream energy capacity could exceed 120 GW globally [1]. Although extracting this total power is not technically feasible, it is estimated by many sources that 75 to 90 GW can be extracted with the different existing technologies [2].

In marine energy industries, particularly in-stream tidal, reliability will be the key. Turbine developers are putting more and more emphasis on pre-deployment testing in order to garner meaningful information on the performance of tidal turbines.

As stated by tidal turbine manufacturers, measuring the performance of a tidal turbine presents two key challenges to the tidal energy industry: 1) prediction in the design stage and 2) verification of the performance once operational [3]. Prediction in the design stage is currently done through small-scale steady-state experimental testing, which uses constant velocity towing tanks [4, 5] or flume tanks [6] to determine power produced and thrust acting on the designed turbine; or a numerical model of the turbine, using constant inlet velocity conditions, over which the flow is simulated using either a simpler blade element/momentum (BEM) [7, 8] method, actuator disks representations [9] or the more powerful and accurate computational fluid dynamics (CFD) methods [10].

These tools have been, and continue to be, used for tidal turbine design, optimization and characterization, easily providing numerous and repeatable data. But recent results presented by Dr. Bjorn Elsaesser's group from Queen's University Belfast showed that the turbine maximum operating power coefficient (C_p) was reduced by 24%, with a consequential reduction in power production of 30%, when comparing turbine operation in a real unsteady tidal flow to steady tests performed by pushing the turbine in still water [11].

The second challenge, verification of the performance once operational, has only been taken on by a select few turbine developers: Alstom through 4 years of careful measurement and testing [3], OpenHydro through years at EMEC [12], and the aforementioned results from the Queen's University group. The latter results point to the fact that most turbine developers, relying on steady tests, might be overestimating their turbine power rating by tens of percent. This could have

an important impact on the overall financial assessment and economic viability of tidal projects. It's therefore important to perform numerical studies using real unsteady velocity conditions to know more precisely the impact of unsteadiness on the turbines performance.

Of the various numerical methods that are employed today for studying turbulent flow over turbines, very few can be employed to study unsteady flow with high enough accuracy. Blade element/momentum (BEM) [7, 8] methods have been shown to be insufficient for unsteady loading [13]. The actuator disc method still lacks the solution quality that would result from a standalone CFD model. A CFD approach has been shown to be capable of resolving turbulence in the near and far field regions at fine resolution for a three dimensional horizontal axis tidal turbine (HATT) [14]. The most commonly used turbulence model in the field of tidal turbine simulation today is the Shear Stress Transport (SST) model. It utilizes k-ω turbulence closure in the inner boundary regions and k-ε closure in the free stream regions, and is capable of resolving turbulence with acceptable margins of error [15, 16].

This shift into unsteady studies has started recently with numerous papers in the last two years looking at various engineering aspects, for example: CFD study of the load on turbine blades stemming from unsteady tidal flow [17], experimental study in a circulating tank of unsteady turbulence (generated artificially using static grids) effect on a small-scale tidal turbine [6, 18, 19]; these studies however used randomly generated flow field and turbulence level. Only one recent conference paper from a team at the University of Manchester (UK) shows the integration of "real tidal" velocity data as the inlet condition of a CFD simulation to properly study the impact of unsteadiness in the flow, in this case using data from the EMEC test site in the Orkney Isles [16].

In Canada, work on characterizing the unsteadiness of tidal flows in the Bay of Fundy has been underway for a few years [20]. Several measurements campaigns have taken place in Grand Passage, Nova Scotia [20, 21, 22]; where it has been demonstrated that standard commercially-available ADCPs can be used to obtain representative estimates of second-order turbulence statistics, including the turbulent kinetic energy and the rate of energy dissipation. High fidelity detached eddy simulations have also been used to characterize the unsteady flow in the Minas Passage [23].

Researchers at Dalhousie University are well positioned to study the impact of unsteady flow on turbine performance using a recently developed CFD model [24]. The numerical methodology was validated against experimental results [4] and used to study turbine wake characteristics [24]. In this paper, the inlet conditions are established based on measurements obtained in Grand Passage, Nova Scotia. The turbine performance and wake dynamics are assessed for a variety of mean flow speeds and tip speed ratios, and comparisons to steady flow simulations are made.

II. Turbine Geometry

The turbine geometry was developed to model the experimental turbine used by Doman *et al.* [5]. TABLE I presents the blade geometry which is based on the NREL S814 airfoil; the overall turbine has a diameter of 762 mm. The axis of rotation is located at 25% of the chord from the leading edge for each cross section. The hub pitch angle for the experimental turbine was measured to be 28 ± 0.875°, 28.875° was used in the numerical model. The nacelle and support structure geometries were estimated from reviews of the publications, dimensions of which are provided in TABLE II. The blade roots and rotor hub were greatly simplified from the experimental setup to facilitate meshing (Fig. 1).

III. Numerical Modelling

A. Fluid Domain

The numerical fluid domain length is based on the dimensions of the Kelvin Hydrodynamics Laboratory tow tank at the Strathclyde University where experimental tests for Doman *et al.*'s turbine were conducted [5].

TABLE I
Blade Parameters [5]

Radius (m)	Twist (°)	Chord (m)
0.089	0	0.0643
0.114	-4.38	0.0629
0.149	-10.74	0.0598
0.183	-14.80	0.0560
0.216	-17.33	0.0516
0.251	-18.91	0.0473
0.286	-19.75	0.0426
0.321	-20.39	0.0381
0.355	-20.87	0.0337
0.381	-21.11	0.0249

TABLE II
Nacelle Geometry Dimensions

Parameter	Dimension
Nacelle Length	1700 mm
Nacelle Diameter	150 mm
Rotor depth	700 mm

Fig. 1 Turbine rendering.

TABLE III
TOW TANK PARAMETERS [5]

Parameter	Magnitude
Length	76 m
Breadth	4.6 m
Height	2.5 m
Maximum flow speed	5 m/s

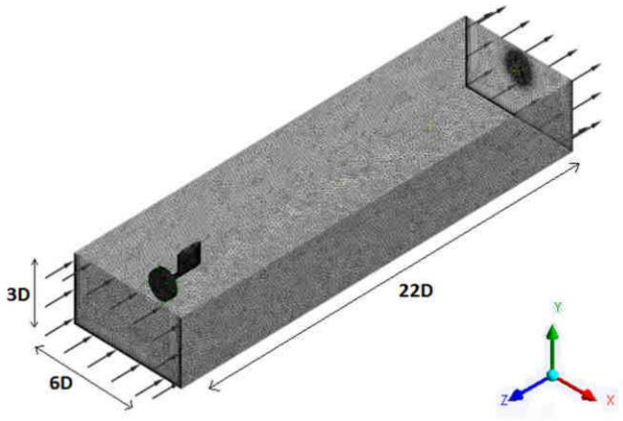

Fig. 2 Fluid domain.

Figure 2 presents the dimensions of the facility. These parameters are represented in the numerical fluid domain with the exception of the domain length. The domain length was shortened to 22*D*, with inlet and outlet lengths of 2*D* and 20*D* respectively, where D = 762 mm denotes the turbine diameter. The fluid domain is shown in Fig. 2 and the turbine is located at (x, y, z) = (0, 0, 0). It has been shown that this length is sufficient as the near wake physics and performance of the turbine is not significantly affected by the outlet domain length [24].

B. Turbulence Models

The k-ω Shear Stress Transport (SST) Reynolds-averaged Navier-Stokes (RANS) turbulence model was chosen to capture turbulent fluctuations in the flow [25]. This is generally accepted as the most suitable turbulence model in similar applications [9, 15, 24]. SST is a two equation eddy viscosity model that employs k-ω in the inner boundary layer and transitions to k-ε in the free stream. SST thereby negates the poor performance of k-ε near solid surfaces and the exaggerated sensitivity of k-ω in free-shear flows [9].

C. Computational Mesh

The fluid domain was spatially discretized using ANSYS Mesher. Unstructured tetrahedrals were used to accurately represent the turbine geometry. The domain consisted of a rotating cylindrical domain encompassing the turbine and a larger stationary domain. Continuity across the interface between the two domains was achieved using the General Grid Interface (GGI).

Several parameters of the mesh were tested to ensure the geometry of the turbine was modelled with enough resolution to accurately capture the its performance. These included the minimum and maximum cell size, curvature normal angle on the blade and growth rate. Special attention was paid to the quality of the inflation layers, where the effect of the first layer height and number of layers were tested [28]. This numerical model was then compared to experimental results performed by Doman *et al.* in the Kelvin Hydrodynamics Laboratory tow tank for validation purposes [5, 28]. A good level of agreement between the numerical and experimental results was shown [28].

Figure 3 provides a detailed view of the turbine surface mesh, and Fig. 4 shows the cross-section of the blade mesh.

D. Boundary Conditions

The domain boundary conditions are provided in Table IV. At the inlet (z = -2*D*), a time- and depth-dependent velocity was imposed where the synthetic data was based on ADCP velocity measurements that were obtained in 2013 at the northern end of Grand Passage, Nova Scotia [22]. The conditions represent a typical flood tide when the mid-depth velocity ranged from 1.8 to 2 m/s.

The total velocity at the inlet was expressed as:

$$V(Y,t) = \bar{V}(Y) + v'(t) \quad (1)$$

where $\bar{V}(Y)$ is the mean velocity profile and $v'(t)$ is the turbulent component.

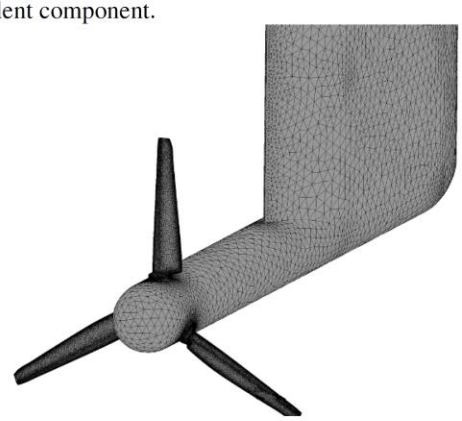

Fig. 3 Detailed view of turbine surface mesh.

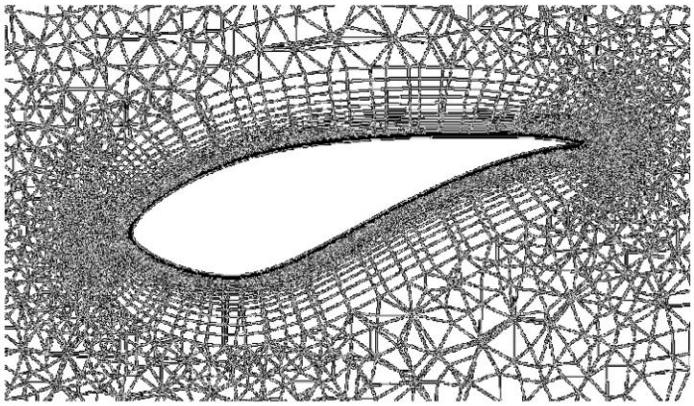

Fig. 4 Cross-section of the blade mesh.

TABLE IV
BOUNDARY CONDITIONS

Boundary	Condition
Inlet	Unsteady Flow with an Averaged Normal Velocity $\bar{V}$= 2.05 m/s
Outlet	P_{rel} = 0 Pa
Tank Walls	No-Slip, Side Wall Velocity = 2.05 m/s Top Surface as a Free Surface
Turbine Walls	No-Slip
Domain Interfaces	Transient Rotor

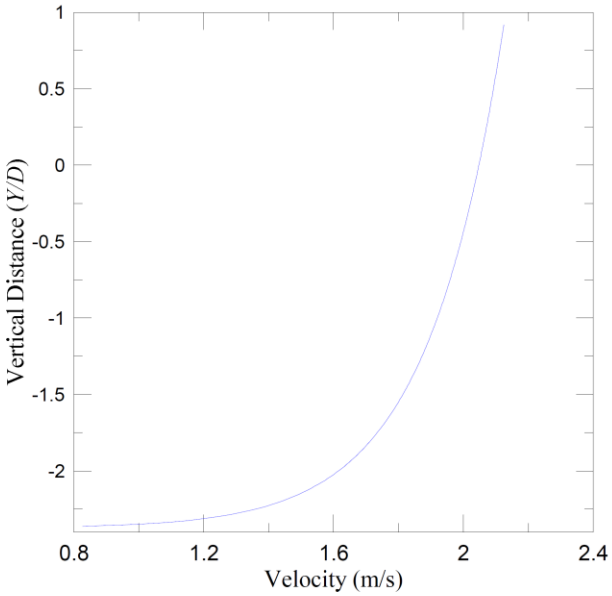

Fig. 6 Mean velocity profile $\bar{V}$ as a function of *Y*.

The mean velocity profile was generated from the law-of-the wall which is given by:

$$\bar{V}(Y) = \frac{v_*}{\kappa}\ln(\frac{Y}{Y_0}) \quad (2)$$

where $\kappa = 0.4$ is the von Karman constant, v_* is the friction velocity and Y_0 is the bottom roughness lengthscale. The v_* and Y_0 parameters are based on the best fit to the ADCP data and are given by v_* = 0.0939 m/s and Y_0 = 0.0037 m. The resulting velocity profile is shown in Fig. 6.

Because an ADCP cannot measure v' directly, the measured dissipation rate of $\varepsilon = 8.6 \times 10^{-5}$ W/kg was used to obtain a realistic turbulent velocity [22]. A synthetic time series was generated by superimposing waves of random phase at wavenumbers below the Kolmogorov microscale, where the amplitude of each Fourier component was such that the theoretical form of the spectral density, *S*, was ensured, *i.e.* $S \sim k^{-5/3}$. In reality, ε and hence v' varies with depth; however, in these initial simulations, v' was independent of *Y*. The 20 s synthetic time series of v' is plotted in Fig. 7 a).

No-slip conditions were applied to every surface in the model, except the top water surface which was simulated as a free surface. The side walls of the simulation domain were given the same average velocity as the inlet flow to limit the impact of the wall on flow dynamics. The rotational rate of the cylindrical domain was set to achieve the desired tip speed ratio (TSR), defined as:

$$TSR = \frac{\omega R}{\bar{V}} \quad (3)$$

where ω is the rotational rate in rad/s, R is the turbine radius (381 mm), and $\bar{V}$ is the reference velocity (constant during the experiment).

In addition, steady state simulations were performed in order to enable the comparison of the wake behaviour. These simulations used only the constant mean velocity profile $\bar{V}(Y)$ as inlet velocity. Two thousand iterations were necessary to reach convergence in the wake.

In these steady simulations, the frozen-rotor quasi-steady approach was used to model the dynamics of the flow (whereas the fully transient-rotor one was used for the transient runs). With the exception of the inlet velocity and the frozen- or transient-rotor approach, all the simulations were performed with the same mesh and boundary conditions. All simulations are performed at constant TSRs.

E. Resolution Procedure

All simulations were performed using between 26 and 30 cores on a Dell Precision T7810, 16 cores (2.4 GHz) hyper threaded with 128 GB of RAM. The computation time varied between 1 hour and 48hours (transient simulations).

IV. NUMERICAL COMPARISON BETWEEN UNSTEADY AND STEADY FLOW

A. Performance Calculation

Power and thrust coefficients are used for comparison. These properties are described as follows:

$$C_t = \frac{T}{\frac{1}{2}\rho A V_A^2} \quad (4)$$

$$C_p = \frac{P_m}{\frac{1}{2}\rho A V_A^3} = \frac{\omega Q}{\frac{1}{2}\rho A V_A^3} \quad (5)$$

where T and P_m are the thrust and mechanical power produced, respectively, ρ is the fluid density, A is the rotor swept area, and Q is the rotor torque.

Because a velocity profile is used at the inflow, velocity varies with depth. Depending on the choice of reference velocity made (mean velocity profile $\bar{V}$ averaged on a swept area, velocity $\bar{V}(Y)$ at a specific location Y_1, etc.), power and thrust coefficients values can differ substantially. As shown by Fleming *et al.*, the power curve may be misrepresented if an incorrect reference velocity is taken [29]. They showed that the correct reference velocity is the one equal to the integral of the velocity over the rotor swept area. Thus, for all thrust and power coefficients computed in this paper, $V_A(t)$ is defined as the integral over the velocity of the rotor swept area.

For the unsteady simulations, total velocity $V_A(t)$ is defined by:

$$V_A(t) = v'(t) + \overline{V_A} \quad (6)$$

Therefore $V_A(t)$ is given at time t_1. Due to the advection time of the fluid from the inlet to the turbine, the inflow velocity at t_1 does not correspond to the fluid's velocity going through the turbine at t_1. To determine the actual velocity at the turbine, a time offset has been added. This offset is equal to the advection time of the fluid from the inlet to the turbine equal to 0.75 s.

Figures 7 a), b) and c) show, respectively, the evolution of V, C_p and C_t as with time. In these figures, TSR is equal to 4 and the average velocity is set to 2.05 m/s. Twenty seconds of 'real data' were used to perform these simulations.

The magnitude of the fluctuations in the C_t is far higher than for C_p: C_p values varying from 0.24 to 0.4 whereas C_t values from 0.08 to 0.95.

This large variation in the C_t values (consequently, also in blade loading) could lead to an increase of the turbine/blade fatigue and stress, possibly reducing the life expectancy of the device.

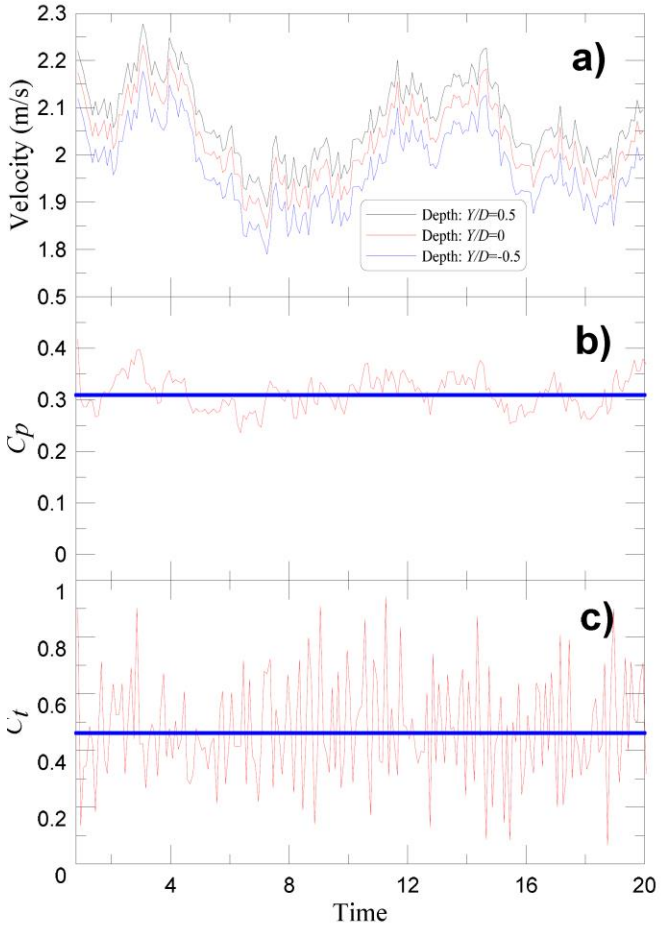

Fig. 7 a) Inlet Velocity as a function of time for 3 different depths: Y/D = 0.5, Y/D = 0 and Y/D = -0.5 (Y/D = 0 corresponds to the hub height) b) C_p, as a function of time and c) C_t as a function of time (blue: coefficient from the steady simulation, red from the transient one).

B. *Power and Thrust Coefficients*

With the inlet velocity being time-dependent in the transient simulations, the instantaneous velocity varies from 1.75 to 2.2 m/s (when the average velocity is 2.05 m/s). Therefore, for comparison, it was decided to perform the steady simulations with the same range of input speeds. Results in Fig. 8 include the results of steady simulations covering a range of tip speed ratios (TSR = 3 – 4.5) and velocities (1.75- 2.2 m/s). Transient simulations cover a range of TSR (3 - 4.5) obtained for one transient inlet velocity having an average of 2.05 m/s. Figure 8 shows the comparative C_p-TSR and C_t-TSR curves for steady and unsteady flow.

Both C_p and C_t follow a similar trend for steady and unsteady simulations. However, in the transient results, the fluctuation amplitude in the C_p and C_t values is much higher than for steady flow results.

The turbine's overall performance for an unsteady flow is comparable to the one obtained for a steady flow. The steady flow C_p curve has an average relative difference of 0.83% and average absolute difference of 0.003 below unsteady simulations values. Likewise, the predicted C_t curve has an average relative difference of 0.07% below unsteady simulations values. As can be seen, the relative difference grows with TSR to reach 0.5% for TSR=4.5.

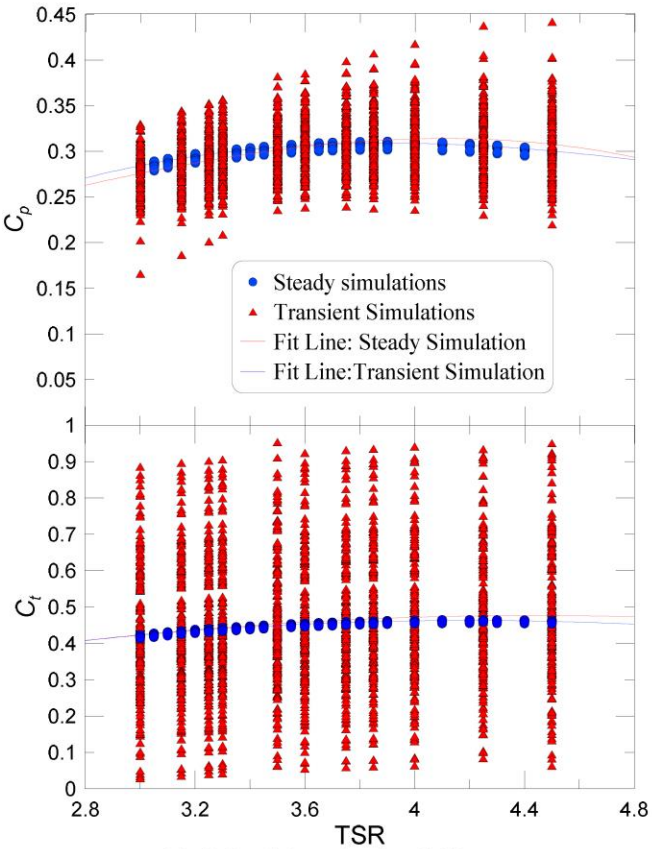

Fig. 8 C_p and C_t as a function of TSR.

V. Results and Discussion

A. Mechanical Performance

Following the presentation of results from Dr. Bjorn Elsaesser's group experiments [11], the mechanical performance of the turbine was assessed. To do so, new simulations were run with changed inlet conditions. Steady simulations covering a wider range of velocities (1.45 to 2.3 m/s) were performed at constant TSRs (3, 3.5 or 4), whereas in the transient simulations, three different velocities (integral of the velocity on the rotor swept area) were used: 1.6, 1.8 and 2.05 m/s. TSR remained constant for the duration of a simulation. The comparison of the mechanical power against inflow velocity for these three TSR-values is shown in Fig. 9.

In each case, the relationship between the mechanical power P_m and the velocity follows the power law expected from Eq. (5). The mechanical power is proportional to the power in the flow and thus the cube of the inflow velocity. The relationship is very consistent for the steady and unsteady flow even if the amount of scatter in the instantaneous P_m values is important for transient results.

Taking a closer look at the curves for each TSR, for TSR = 3.5, the unsteady tests mechanical performance is always lower than the steady one: approximately 7 W (3.3%) less than the steady tests at 1.45 m/s and 27.7 W (3.3%) less than the steady tests at 2.3 m/s. For TSR = 3 or 4, the difference between the steady and the transient mechanical performance depends on the velocity-value. For TSR = 3, the difference is close to 0 at 1.45 m/s and equal to 50 W (6.3%) and the opposite trend is seen for TSR = 4.

B. Wake Characteristics

Velocity deficit and turbulence intensity were computed in order to visualize what is happening in the wake, and are defined as:

$$V_{deficit} = 1 - \frac{V_W}{\bar{V}_A} \tag{7}$$

$$TI = \frac{100}{\bar{V}_A}\sqrt{\frac{2}{3}k} \tag{8}$$

where V_W is the local wake velocity and k is the turbulent kinetic energy. $\bar{V}_A$ is the time average of the integral of the velocity over the rotor swept area and therefore remains constant for the duration of the simulation (so no time offset was added to consider the advection time from the inlet to the turbine even for transient simulations).

To visualize clearly what is happening in the wake, dimensionless velocity (V/V_0) are plotted in Fig. 10 at different locations along the wake, both for steady and transient simulations. Because in transient simulations, the wake is constantly evolving, results only for a single specific time value are presented. This was chosen to be 20 s because it is a good compromise between the time needed to obtain a fully developed wake which can be observed to take approximately 10 s, and a simulation which lasts for too long.

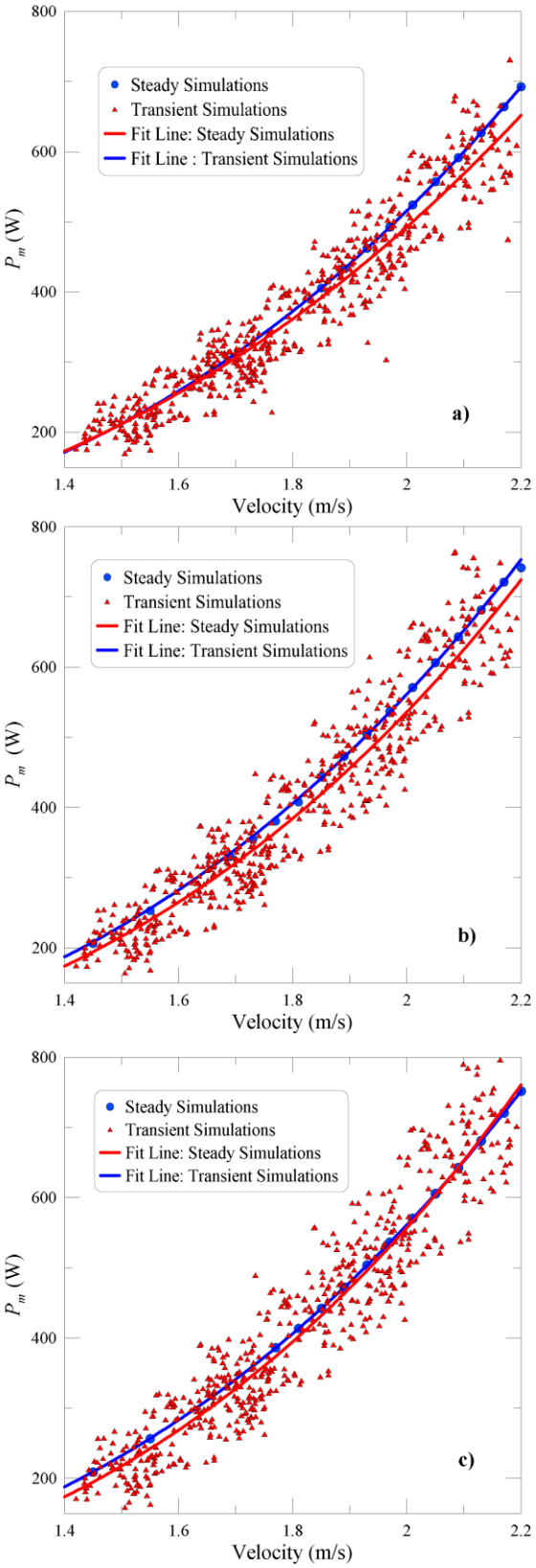

Fig. 9 Steady and transient mechanical power against inflow velocity for: a) TSR = 3, b) TSR = 3.5 and c) TSR = 4.

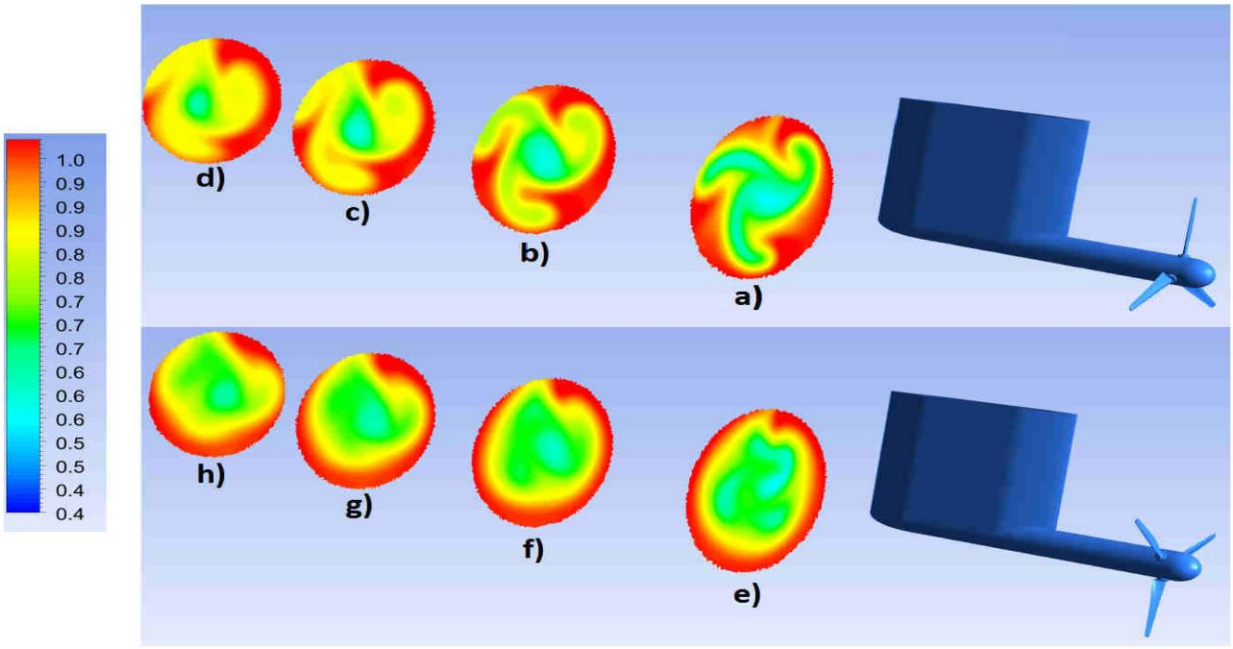

Fig. 10 Normalized Velocity V/V_0 for steady simulations at a) 3D, b) 5D, c) 7D and d) 9D and transient simulations at e) 3D, f) 5D, g) 7D and h) 9D.

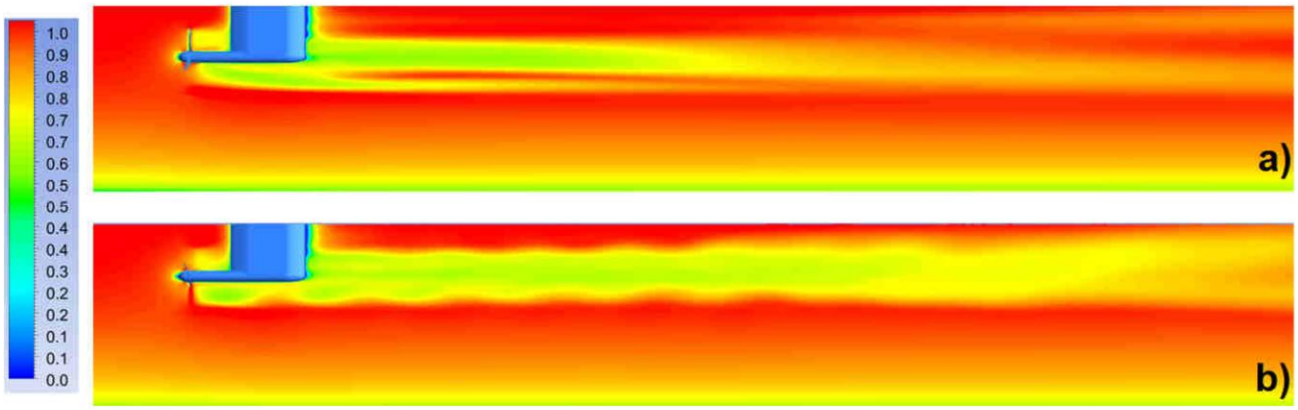

Fig. 11 Normalized Velocity V/V_0 on mid-vertical plane for a) steady flow, b) transient flow at t = 20 s.

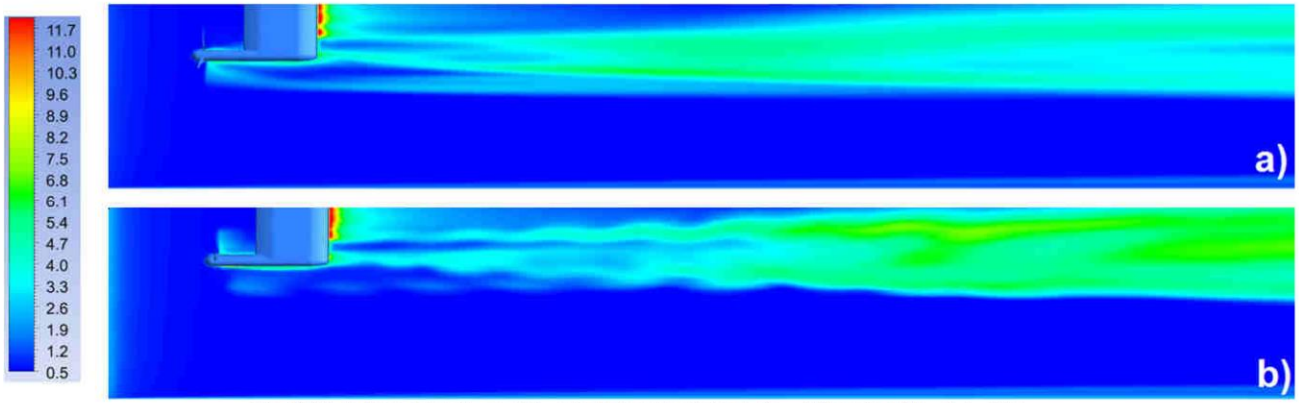

Fig. 12 Turbulence intensity on mid-vertical plane for a) steady flow, b) transient flow at t = 20 s.

The shape of velocity profile through the wake is different: a cylindrical-shaped wake for transient flow whereas there is a "turbine-shaped" wake for steady simulations. Moreover, the velocity deficit seems to disappear faster in the constant velocity simulations. Figure 10 a), b), c) and d) also illustrates the effects, of the fixed rotor blades in the steady simulation. In contrast, in transient simulations, with the Transient Rotor approach, the blades are always moving. That is why a large circle profile can observe in the transient simulation.

Figure 11 represents the normalized velocity on mid-vertical plane. It shows that the velocity deficit is more important for transient simulations in the far field wake (7*D* and 9*D*) but it is the opposite in the near field. As mentioned earlier, depending on the type of inflow velocity used, the shape of the wake is different. The wake is wider for the turbulent simulation and disappears more slowly. At a distance of 10*D*, velocity is approaching the inflow velocity for steady state whereas the velocity deficit is still important in the second case. Even at a distance of 20*D*, the flow is still affected by the turbine in the transient case.

Figure 12 presents the turbulence intensity along the centre plane of the wake. Unlike velocity profiles, turbulence intensity profiles are much the same in both cases: turbulence is still significant at a distance of 20*D* and increases as moving away from the turbine. When turbulence intensity is lower than 4% in the near wake, it is approximately 6% at a distance of 20*D*. As above, turbulence is higher in the transient case, especially in the far wake: at a distance of 20*D*, maximum turbulence intensity is 3.6% for constant flow simulations and 5.7% for the unsteady simulation. This may due to the large fluctuation of the inlet velocity during the simulation.

Figures 13 and 14 present the values of turbulence intensity and velocity deficit over horizontal lines and vertical lines at 5*D*, 10*D*, 15*D* and 20*D*. First, both for velocity deficit and turbulence intensity, there is no symmetry along *Z*. In steady simulation, this is due to the Frozen Rotor approach which forces the fluid to twist around the blades. That twist is always generated in the same side of the blade and thus it creates a deflection at *X/D*= -0.5 as seen in Figs. 13 and 14 b)-c)-d). At 5*D*, irregularities in the turbulence intensity can be observed at $x/D = 0$ and $\pm$ 0.5 (especially in the transient simulations). These irregularities correspond to the turbulence due to root and tip losses, and nacelle structure interaction.

Regarding the velocity deficit, the wake seems to become wider from 5*D* to 20*D*, both in the horizontal and vertical directions. The velocity deficit is not confined anymore between -0.5 and 0.5 m (in both directions at 5*D*) but between -0.75 and 0.9 m (vertical direction at 20*D*). The results demonstrate also that average velocity deficit is higher in the transient simulations than steady simulations and so the velocity deficit disappears faster in the constant velocity simulations. For example, the average velocity deficit is approximately 0.09 at a horizontal distance of 10*D* for a constant velocity inflow and 0.15 for transient simulations. However, velocity deficit in constant velocity simulations seems to be over-predicted outside of the wake.

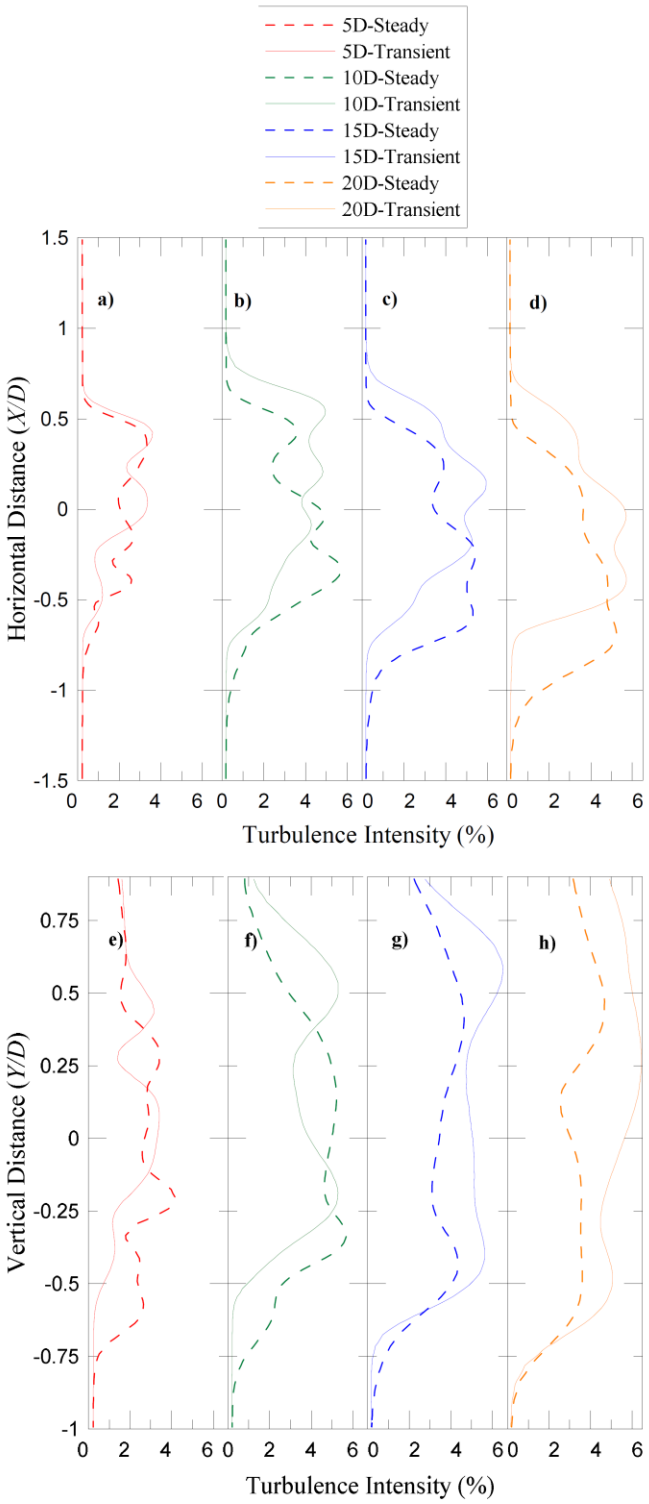

Fig. 13 Turbulence intensity: a) Horizontal - 5*D*, b) Horizontal - 10*D*, c) Horizontal - 15*D*, d) Horizontal - 20*D*, e) Vertical - 5*D*, f) Vertical - 10*D*, g) Vertical - 15*D*, h) Vertical - 20*D*.

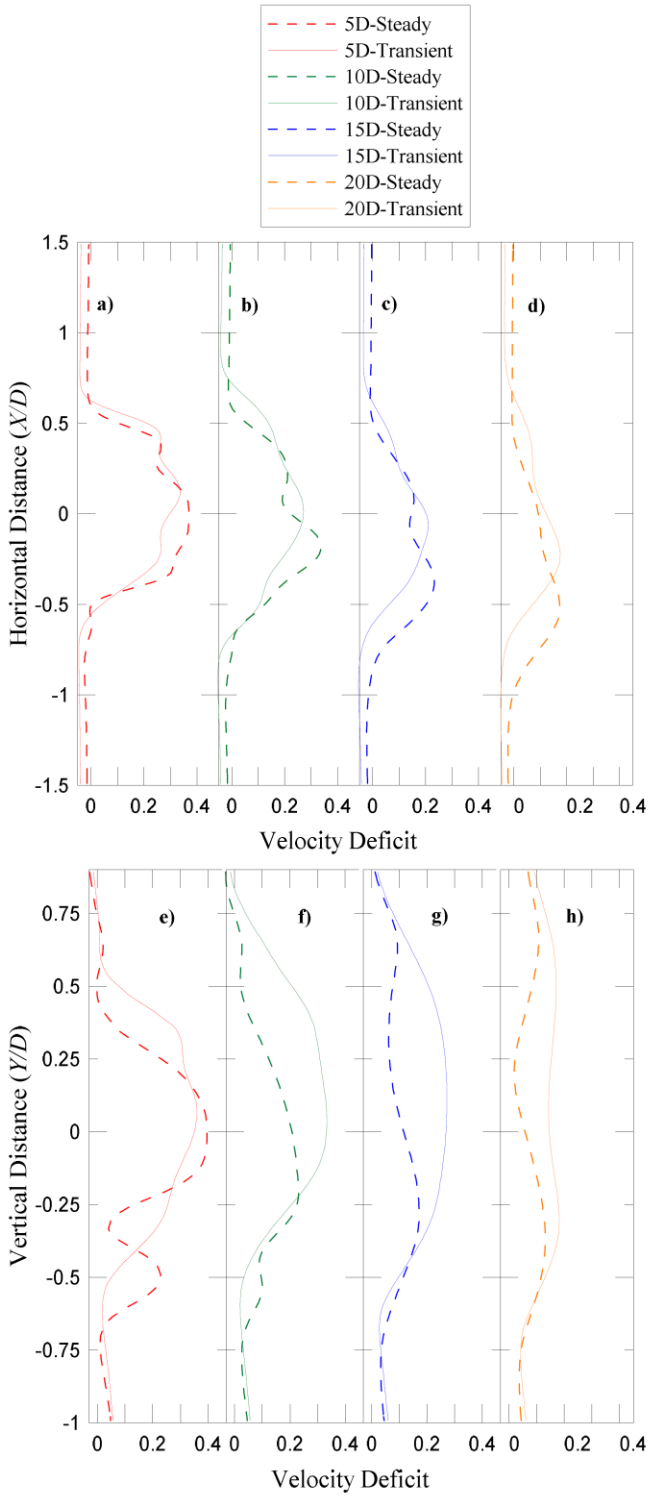

Fig. 14 Velocity deficit: a) Horizontal - 5*D*, b) Horizontal - 10*D*, c) Horizontal - 15*D*, d) Horizontal - 20*D*, e) Vertical - 5*D*, f) Vertical - 10*D*, g) Vertical - 15*D*, h) Vertical - 20*D*.

Regarding turbulent intensity, results may be difficult to interpret: for turbulence intensity as a function of vertical distance, turbulence is higher for transient results than steady one. For instance, at a distance of 15*D*, average turbulence intensity is approximately 3% for steady state simulations and 4% for transient. However, it is not so obvious when looking to turbulence as a function of horizontal distance *e.g.* at a distance of 20*D*, average turbulence intensity is equal to 1.7% for transient flow and 1.9% for steady flow simulations. It can also be seen that turbulence increases from 5*D* to 20*D* in both directions.

VI. Conclusions

A numerical model of a three bladed horizontal axis tidal turbine under realistic turbulent tidal flow has been created. The preliminary results of this investigation have been compared with steady flow numerical model results with good agreement in trends. Prediction of both C_p and C_t are very similar in both cases. These similar trends observed in both C_p and C_t curve are important as they indicate that the appropriate flow physics are being accounted for. Only TSR values related to maximum C_p and C_t changed. For C_p curves, tip speed ratio is approximately equal to 3.9 in steady flow and 4.1 for transient conditions. In transient flows, this results however in an approximate 4% reduction in performance (for TSR = 3.5), though there is increased uncertainty due to the levels of scatter in the numerical data points.

Velocity deficit plots show the wake is wider in transient simulations than steady ones. The velocity deficit disappears also faster in the constant velocity simulations. Turbulent effects in the wake seem to increase after a distance of 10*D* downstream of the turbine in this setup, as shown in Fig. 14. These turbulence effects are higher in the transient simulations.

This comparative analysis of numerical steady and transient simulations show the impact of the unsteadiness of realistic tidal flows on the performance of tidal turbines. In view of the above, the current use of steady state testing (numerical or experimental) for design stage can be questioned. The observed changes in the wake's characteristics and the high variations of the loads on the blades (reference to *Ct*-curve as a function of time) must also be better assessed.

Acknowledgment

The authors are grateful to the Offshore Energy Research Association (OERA) of Nova Scotia and the Canadian Foundation for Innovation (CFI) for their financial support for this work.

References

[1] (2014) The Marine Current Turbines website. [Online]. Available: http://www.marineturbines.com/

[2] (2016) The Atlanted Resources website [Online]. Available: http://atlantisresourcesltd.com/marine-power/global-resources.html

[3] J. McNaughton, S. Harper, R. Sinclair, B. Sellar, "Measuring and Modeling the Power Curve of a Commercial-Scale Tidal Turbine" in *The 11th European Wave and Tidal Energy Conference*, 2015.

[4] A. S. Bahaj, A.F. Molland, J.R. Chaplin, W.M.J. Batten, "Power and thrust measurements of marine current turbines under various hydrodynamic flow conditions in a cavitation tunnel and a towing tank" in *Renewable Energy*, 32, pp. 407-426, 2007.

[5] D. Doman, R.E. Murray, M.J. Pegg, K. Gracie, C.M. Johnstone, T. Nevalainen, "Tow-tank testing of a 1/20th scale horizontal axis tidal turbine with uncertainty analysis" in *International Journal of Marine Energy*, 11 pp. 105-119, 2015.

[6] P. Mycek, B. Gaurier, G. Germain, G. Pinon, E. Rivoalen, "Experimental study of the turbulence intensity effects on marine current turbines behavior. Part I: one single turbine" in *Renewable Energy*, 66, pp. 729-746, 2014.

[7] W.M.J. Batten, A.S. Bahaj, A.F. Molland, J.R. Chaplin, "The prediction of the hydrodynamic performance of marine current turbines" in *Renewable Energy*, 33, pp. 1085-1096, 2014.

[8] A. S. Bahaj, W.M.J. Batten, G. McCann, "Experimental verifications of numerical predictions for the hydrodynamic performance of horizontal axis marine current turbines" in *Renewable Energy*, 32, pp. 2479-2490, 2007.

[9] M.E. Harrison, W.M.J. Batten, L.E. Myers, A.S. Bahaj, "A comparison between CFD simulations and experiments for predicting the far wake of horizontal axis tidal turbines" in *The 8th European Wave and Tidal Energy Conference*, 2009.

[10] C.H. Jo, J.H. Lee, Y.H. Rho, K.H. Lee, "Performance analysis of a HAT tidal current turbine and wake flow characteristics" in *Renewable Energy*, 65, pp 175-182, 2014.

[11] P. Jeffcoate, B. Elsaesser, T. Whittaker and C. Boake, "Testing Tidal Turbine – Part 1: Steady Towing Tests vs. Tidal Mooring Tests" in *International Conference on Offshore Renewable Energy*, 2014.

[12] P. Muller, F. Sainclair, A. Carlisle, C. Delafosse, "Tidal Current Turbine Optimization using CFD Simulation" in the *11th European Wave and Tidal Energy Conference*, 2015.

[13] J.H. Lee, S. Park, D.H. Kim, S.H. Rhee, M.-C. Kim, "Computational methods for performance analysis of horizontal axis tidal stream turbines" in *Applied Energy*, 98, pp. 512-523, 2012.

[14] T. O'Doherty, A. Mason-Jones, D.M. O'Doherty, C.B. Byrne, I. Owen, Y.X. Wang, "Experimental and Computational Analysis of a Modal Horizontal Axis Tidal Turbine" in *The 8th European Wave and Tidal Energy Conference*, 2009, p. 1085-1096.

[15] R. McSherry, J. Grimwade, I. Jones, S. Mathias, A. Wells, A. Mateus, "3D CFD modelling of tidal turbine performance with validation against laboratory experiments" in *The 9th European Wave and Tidal Energy Conference*, 2011.

[16] U. Ahmed, I. Afgan, D.D. Apsley, T. Stallard, P.K. Stansby, "CFD Simulations of a Full-Scale Tidal Turbine: Comparison of LES and RANS with Field Data" in *the 11th European Wave and Tidal Energy Conference*, 8p, 2015.

[17] X. Wang, A.H. Day, "CFD Turbulence Modelling of Tidal Turbine Unsteady Blade Load" in *the 11th European Wave and Tidal Energy Conference*, 10 p., 2015.

[18] T. Blackmore, B. Gaurier, L. Myers, G. Germain, A.S. Bahaj, "The Effect of Freestream Turbulence on Tidal Turbines" in *the 11th European Wave and Tidal Energy Conference*, 8 p., 2015.

[19] P. Mycek, B. Gaurier, G. Germain, G. Pinon, E. Rivoalen, "Experimental study of the turbulence intensity effects on marine current turbines behavior. Part II: two interacting turbines" in *Renewable Energy*, 68, pp. 876-892, 2014.

[20] A.E. Hay, J. McMillan, R. Cheel, D. Schillinger, "Turbulence and Drag in a High Reynolds Number Tidal Passage targeted for In-stream Tidal Power" in the *IEEE Oceans'13*, 2013.

[21] J.M. McMillan, A.E. Hay, R.G. Lueck, and F. Wolk, "An Assessment of the Dissipation Rates at a Tidal Energy Sites using a VMP and an ADCP", in the *11th European Wave and Tidal Energy Conference*, 8 p, 2015.

[22] J.M. McMillan, A.E. Hay, R.G. Lueck, and F. Wolk, "Rates of dissipation of turbulent kinetic energy in a high Reynolds number tidal channel" in Journal of Atmospheric and Oceanic Technology, 33, pp 817 -- 837, 2016.

[23] K.W. Wilcox, I. McLeod, A. Gerber, T. Jeans, J. Culina, "Validation of High-Fidelity CFD Simulation of the Unsteady Turbulent Tidal Flow in Minas Passage" in the *11th European Wave and Tidal Energy Conference*, 13 p, 2015

[24] N. Osbourne, D. Groulx, and I. Penesis,"3D Modelling of a tidal turbine – a numerical investigation of wake phenomena" in *the 11th European Wave and Tidal Energy Conference*, 10p, 2015.

[25] F. Menter, "Tow-equation eddy-viscosity turbulence models for engineering applications" in *AIAA Journal*, pp. 1598-1605, 1994.

[26] I. Afgan, J. McNaughton, S. Rolfo, D.D. Apsley, T. Stallard, P. Stansby, "Turbulent flow and loading on a tidal stream turbine by LES and RANS" in *International Journal of Heat and Fluid Flow*, pp. 96-108, 2013.

[27] J. McNaughton, S. Rolfo, D. Apsley, I. Afgan, T. Stallard, P. Stansby, "CFD Prediction of Turbulent Flow on an Experimental Tidal Stream Turbine using RANS modelling" in *The 1st Asian Wave and Tidal Energy Conference Series*, 2012.

[28] G. Currie, N. Osbourne and D. Groulx, "Numerical Modelling of a Three-Bladed NREL S814 Tidal Turbine" to be published and presented at AWTEC 2016 in October 2016.

[29] C.F. Fleming, S.C. McIntosh, R.H.J. Willden, "Tidal turbine performance in sheared flow" in *The 10th European Wave and Tidal Energy Conference*, 2013.

Appendix B

AORES 2016 – Abstract

Numerical Modeling of Tidal Turbine Behaviour under Real Turbulent Tidal Flow Conditions

Tanguy Leroux, Nicholas Osbourne, Dominic Groulx*

Department of Mechanical Engineering, Dalhousie University, Halifax, Canada

Keywords: Tidal Turbine Wake Recovery, CFD Study, Frozen Rotor Approach, Transient Simulations

A numerical study looking into the simulated wake behind a three-bladed horizontal axis tidal turbine (HATT) is currently underway; results of that study will be presented during AORES. For the purpose of this study, the experimental results from the HATT used by the French research groups at l'Institut Français de Recherche pour l'Exploitation de la MER (IFREMER) and the Laboratoire Ondes et Milieux Complexes (LOMC) at the Université du Havre are used. The IFREMER-LOMC turbine uses NACA 63418 profile blades having a radius of 350 mm and the experiments were performed in the IFREMER flume tank situated in Boulogne-Sur-Mer (usable section being 18 m long, 4 m wide and 2 m deep). Both C_p and C_T were obtained for the turbine, as well as velocity deficit at numerous section downstream of the turbine; results provide in Paul Mycek PhD thesis titled "Étude numérique et expérimentale du comportement d'hydroliennes".

The wake from the turbine is studied numerically in this work, and compared to the experimental results. The impact of various parameters in geometry build and numerical setup is discussed. All results provided incorporate the Reynolds Averaged Navier Stokes (RANS) Shear Stress Transport (SST) turbulence model. Simulations cover a range of tip speed ratios and a constant inflow velocity of 1 m/s. The resulting power and thrust coefficients, C_p and C_T, are compared to experimental results for validation purposes. The results show a good level of agreement. Results of a wake mesh convergence study are also provided when it comes to the turbine wake velocity deficit.

Two families of simulations are performed in ANSYS CFX, using either the frozen-rotor quasi-steady approach, or the fully transient one. This study will look at differences in wake resolution and behaviour obtained from both approaches in order to garner meaningful information on which numerical methods should be used in wake studies. This work is sponsored in part by the Offshore Energy Research Association (OERA) of Nova Scotia.